Yang et al., 1995a). Recent studies revealed that EAT inhibits apoptosis in vitro and in vivo (Akgul et al., 2000a,b; Ando et al., 1998; Matsushita et al., 1999; Moulding et al., 2000; Reynolds et al., 1994; Sano et al., 2001, 2000).

The in vivo effects of Bcl-2 related genes have been investigated in transgenic or knock-out mice. Bcl-2 transgenic mice are known to promote cell survival in B cells, T cells and thymocytes (McDonnell et al., 1989; Sentman et al., 1991; Siegel et al., 1992; Strasser et al., 1991). Mice deficient for bcl-2 display increased apoptosis in selected tissues (Veis et al., 1993). These phenotypes reflect the anti-apoptotic functions established for bcl-2 in vitro. On the other hand, bax transgenic mice present with increased apoptosis in T cells and mice deficient for bax demonstrate hyperplasia of thymocytes and B cells (Brady et al., 1996a,b; Knudson et al., 1995). Male Bax-deficient mice are infertile with atrophic adult testes and an empty epididymis and vas deferens; a complete cessation of mature sperm cell production occurs in these mice (Knudson et al., 1995). These phenotypes result from the pro-apoptotic functions of Bax.

We generated three lines of EAT transgenic mice, driven by the EF1α promoter, to investigate in vivo the role of EAT during development. Our aim was to determine whether overexpression of the hEAT gene would cause anti-apoptotic effects in vivo similar to the bcl-2 gene. In this report, we show that EAT transgenic mice develop islet cell hyperplasia reflecting inhibition of apoptosis of β cells.

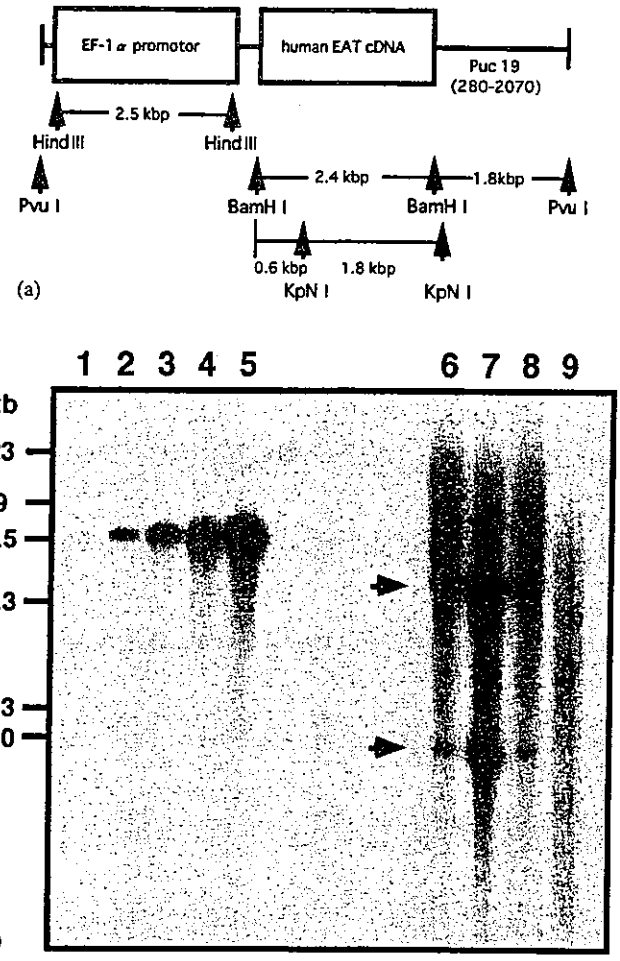

Fig. 1. Generation of EAT transgenic mice. (A) Schema of the EF1α–hEAT (EF1α–EAT) transgene construct. The PvuI fragment was used as the transgene. The same 6.7 kb PvuI fragment was used as a probe for Southern blot hybridization. This hEAT transgene, driven by the EF1α promoter, was injected into the fertilized eggs. (B) Southern blot analysis of tail DNA from heterozygote transgenic lines. The copy numbers of the transgene per diploid genome for each line are: 20 (E2), 150 (E3), and 20 (E12), as shown in lane 6–8, respectively. KpnI-digested tail genomic DNA was hybridized with a ^{32}P-labeled EF1α–EAT probe. Kilobase size markers are shown on the left. Arrows indicate the bands of EF1α–EAT DNA fragments digested with KpnI. Orientation of the hEAT transgene was determined to be head-to-tail in all lines. Lanes 1–5 represent controls for transgene fragment copy numbers (lane 1: 1 copy, lane 2: 10 copies, lane 3: 20 copies, lane 4: 50 copies, lane 5: 100 copies). Lane 9 represents a non-transgenic control.

2. Materials and methods

2.1. Generation of transgenic mice for hEAT gene

To generate transgenic mice that express hEAT, a transgene was constructed with the human EF1α promoter linked to hEAT (EF1α–EAT) (Hanaoka et al., 1991) (Fig. 1A). The PvuI fragment of EF1α–EAT (6.7 kb) was purified and dissolved in 10 mM Tris, 0.25 mM EDTA (pH 7.4) at a concentration of 3 μg/ml. The production of transgenic mice was performed according to standard procedures (Hogan et al., 1986). In brief, a DNA solution (3 μg/ml) was microinjected into the male pronuclei of fertilized mouse eggs taken from superovulated B6C3F1 (C57BL/6 × C3H/He) females. The injected eggs were surgically transferred to the oviducts of B6C3F1 pseudopregnant female mice. Transgene-bearing mice were selected by Southern blot analysis of tail DNA (10 μg) hybridized with the EF1α–EAT probe of the 6.7-kb PvuI–PvuI fragment. Orientation of the transgene integrated into the chromosome and copy numbers of each line were analyzed by Southern blot hybridization. Copy numbers were calculated by the bio-imaging analyzer (BAS2000, Fuji Film, Japan), using the transgene fragment mixed with mouse genomic DNA as copy number controls. The founder mice obtained were assigned with a number preceded with a letter E, like E2 or E3. Offsprings were screened by detecting the 1097-bp hEAT fragment in the tail DNA with polymerase chain reaction (PCR) using a set of appropriate primers. The sequences of the primers used were as follows; the sense primer: 5′ CTGCATCGAACCATTAGCAG 3′, and the antisense primer: 5′ TACAACCAGTCTGCATACAG 3′.

Animals were housed in micro-isolation cages on wood shavings and observed daily for evidence of weakness. The study was approved by the Keio University School of Medicine Care of Experimental Animals Committee.

2.2. Expression of the hEAT transgene compared to endogenous mEAT

Langerhans islets were isolated by collagenase digestion method (Gotoh et al., 1985; Lacy and Kostianovsky, 1967). RNA extraction from islets and other tissues were performed using ISOGEN (Wako, Osaka, Japan), following the manufacturer's instructions. First strand cDNA synthesis was performed using First-Strand cDNA Synthesis Kit (Pharmacia Biotech, Uppsala, Sweden). The PCR reaction was carried out using the synthesized cDNA in a reaction with 50 pmol of each primer and 2.5 Units of Taq DNA polymerase (Toyobo, Osaka, Japan) in a buffer containing 10 mM Tris–HCl (pH 8.3), 50 mM KCl, 2.5 mM $MgCl_2$, 0.1% TritonX-100, and each deoxyribonucleoside triphosphate at 100 μM. The reaction mixtures were then amplified through 35 cycles at 95 °C for 2 min, 48 °C for 1 min, and 72 °C for 1 min, followed by a final extension cycle at 72 °C for 5 min. The primer pairs which detected both hEAT transgene and endogenous mEAT separately are; sense: 5′ CATCGAACCATTAGCAG 3′, and antisense: 5′ GAGCACTTTTCCCATGTATT 3′.

β-actin cDNA was amplified as a control for RNA integrity. The primers used for the β-actin reaction to amplify a 729-kb fragment were; sense: 5′ GTCCCTGTATGCCTCTGGTCGTAC 3′, and antisense: 5′ GCAGCTCAGTAACAGTCCGCCTAG 3′. The PCR amplifications were carried out in an automated thermal cycler (Minicycler, MJ Research, Inc., MA, USA). After electrophoresis of PCR products, the gel was stained with vistra green (Amersham, Buckinghamshire, England) and the DNA bands were visualized using the Fluor Imager (Molecular Dynamics Inc., CA, USA).

2.3. Comparison of the expression level for hEAT in islets of all three lines

Langerhans islets of all three transgenic lines were isolated and RNA extraction from islets was performed. After synthesizing first strand cDNA, the PCR reaction was carried out using the synthesized cDNA through 20 cycles (at 94 °C for 2 min, at 50 °C for 2 min, at 72 °C for 2 min) using an automated thermal cycler (Minicycler, MJ Research, Inc.). The primer pair which specifically detects hEAT but does not detect endogenous mEAT is; sense: 5′ ATTGATTACCCGCCGAA 3′, and antisense: 5′ GGTCAAATGGAAGGAAC 3′.

β-actin cDNA was amplified as a control for RNA integrity. After electrophoresis of PCR products, the gel was stained with vistra green (Amersham) and the DNA bands were visualized using the Fluor Imager (Molecular Dynamics Inc.).

2.4. Differential hybridization of Atlas™ Mouse cDNA expression arrays

Transgenic islets were isolated from a 8-month-old mouse of the E2 line and non-transgenic islets were isolated from a 3-month-old non-transgenic mouse. RNA extraction was performed using ISOGEN (Wako). Universal Ribo Clone cDNA synthesis system (Promega, WI) was used for the first and second cDNA strand synthesis. RNA suspended in 9.4 μl nuclease-free water was mixed with 1 μl CDS primer (0.02 μM; Clontech, Palo Alto, CA). RNA and the primer mix were incubated at 70 °C for 5 min, then at 50 °C for 2 min. Four microliter of 5 × First Strand buffer, 1 μl of RNasin Ribonuclease Inhibitor (40 Units/μl), 2.5 μl of Sodium Pyrophosphate (40 mM) and 1.5 μl of AMV Reverse Transcriptase (20 Units/μl) were added to the reaction mixture on ice and incubated at 42 °C for 4 h. The dsDNA was treated to synthesize blunt ends and 0.4 μl of T4 DNA Polymerase was added followed by incubation at 37 °C for 10 min. The free primer was removed by MicroSpin S-400 column (Amersham Pharmacia Biotech, Sweden).

Blunt ended cDNAs were ligated, for 15 h at 15 °C, to a specially designed linker-primer, 'LL-RI' (Ko et al., 1990a):

LL-RIA: 5′ GAGATATTAGAATTCTACTC-3′
LL-RIB: 3′-TATAATCTTAAGATGAGp-5′

Since the protruding end is not adhesive, a single molecule of the linker was attached to each end of the cDNA in an orientation-specific manner (thus called 'lone linker') (Ko et al., 1990a). Amplification of the cDNA fragments was then performed by PCR through 20 cycles (at 94 °C for 2 min, at 50 °C for 2 min, at 72 °C for 2 min) using an automated thermal cycler (Minicycler, MJ Research, Inc.). Free primer was removed by MicroSpin S-400 column (Amersham). Amplified cDNA was labeled with 50 μCi [α-^{32}P] dCTP (3000 Ci/μmole) using a random primer labeling kit (Amersham). The free ^{32}P was removed by Sephadex G-50 column (Amersham).

Equal amounts of labeled cDNA (1×10^8 cpm) from transgenic and non-transgenic islets were then hybridized to two Atlas™ Mouse cDNA expression arrays in 5 ml of hybridization solution for 18 h at 65 °C. The expression arrays were washed in solution 1 (2 × SSC and 1% SDS) for 60 min at room temperature. A second wash was performed at 65 °C for 40 min in solution 2

(0.1 × SSC and 0.5% SDS). The filters were then exposed on Imaging plates (Fuji Film) for 48 h and analyzed by BAS 2000 (Fuji Film).

2.5. Histology

For routine histology, pancreatic tissue was fixed in 10% formalin and embedded in paraffin. Sections (6 μm) were processed and stained with hematoxylin and eosin. All cases that demonstrated islet cell hyperplasia and several cases with normal islets were then serially sectioned for immunohistochemistry. Immunohistochemical staining was performed with a guinea pig anti-insulin antibody (DakoCytomation Co. Ltd., Copenhagen, Denmark) and a rabbit anti-glucagon antibody (Dako).

2.6. Quantitative area measurement of islets

For quantitative area measurement of islets, we used the MAC SCOPE (Mitani, Inc., Chiba, Japan) software program for analysis. For analysis, 1 randomly sectioned slide from each paraffin block, representing a single animal, was used. The area to be measured by the MAC SCOPE (1–3 mm^2) was chosen to include the maximal islet detected on the slide. From this chosen area, the ratio of the islet cell to the pancreatic area was measured.

2.7. Measurement of glucose and insulin

Mice were fasted overnight and glucose was administered intraperitoneally at 2 mg glucose/g body weight (BW). Fifteen minutes after glucose administration, blood was collected from the right cardiac ventricle to measure blood glucose and serum insulin levels. Blood glucose was measured immediately using whole blood by the Advantage (Yamanouchi Co., Ltd, Tokyo, Japan) kit. Serum insulin levels were measured by EIA using the ELSIA-F-Insulin (International Reagents Corporation, Kobe, Japan) kit and human insulin standards.

In the insulin tolerance test, human insulin (0.5 Units/kg) was injected intraperitoneally in anesthetized adult mice (5–8 months) after fasting overnight. Blood samples were taken from the tail vein.

All assays were performed in duplicate.

2.8. Statistical analyses

Descriptive statistics, ANOVA followed by Bonferroni/Dunn test and regression analysis, were performed. A P value less than 0.05 denoted the presence of a statistically significant difference.

3. Results

3.1. Generation of EAT transgenic mice

We generated several lines of EAT transgenic mice. The EAT gene was driven by the EF1α promoter (Fig. 1A). Initial screening was carried out by Southern blot analysis of tail DNA using an EF1α–EAT probe; mice incorporating the integrated gene were determined by positive hybridization signals (Fig. 1B). The transgene is observed to be intact in each line and is integrated in a head-to-tail fashion in all lines. The copy number, as determined by phosphoimaging, was 20 for the E2 line, 150 for the E3 line and 20 for the E12 line. All three founder animals were subsequently bred with F1 (C57BL/6 and C3H/He) animals and offsprings heterozygous for the transgene were screened by PCR.

3.2. Analysis of hEAT expression

Offsprings from the three original founders—designated E2, E3, and E12—were found to express the hEAT transgene ubiquitously in tissues including the liver, kidney, heart, lung, pituitary gland, and Langerhans islets by RT-PCR, although expression levels varied among tissues. Comparison of hEAT transgene expression with endogenous mEAT expression showed that Langerhans islets exhibited higher expression levels of hEAT transgene compared to other tissues (Fig. 2A).

We next analyzed hEAT expression in Langerhans islets of all three transgenic lines by RT-PCR. As shown in Fig. 2B and C, the expression level in the E2 line was much higher than in the other two lines. The expression level (hEAT/β-actin) was lowest in the E3 line; however, the difference between the E3 and E12 lines was subtle.

The expression of the transgene was found to be below levels detectable by Northern blot analysis. This is not due to the construct of the transgene as the same transgene is expressed at high levels in cultured fibroblast clones as determined by RNA blot analysis (Sano et al., 2001). Nevertheless, transgenic mice which express EAT at high levels may possibly be lethal during embryogenesis.

3.3. Enlargement of islets in EAT transgenic mice

Histological examination revealed enlargement of pancreatic Langerhans islets of EAT transgenic mice compared with non-transgenic mice (Fig. 3A–C). To determine the functional composition of these enlarged lesions, we performed immunohistochemical analysis with antibodies to insulin and glucagon. The majority of the cells were positive for insulin while cells positive for glucagon were observed only sporadically (Fig. 3D and E). The same immunohistochemical pattern was observed in all the three transgenic lines produced. The

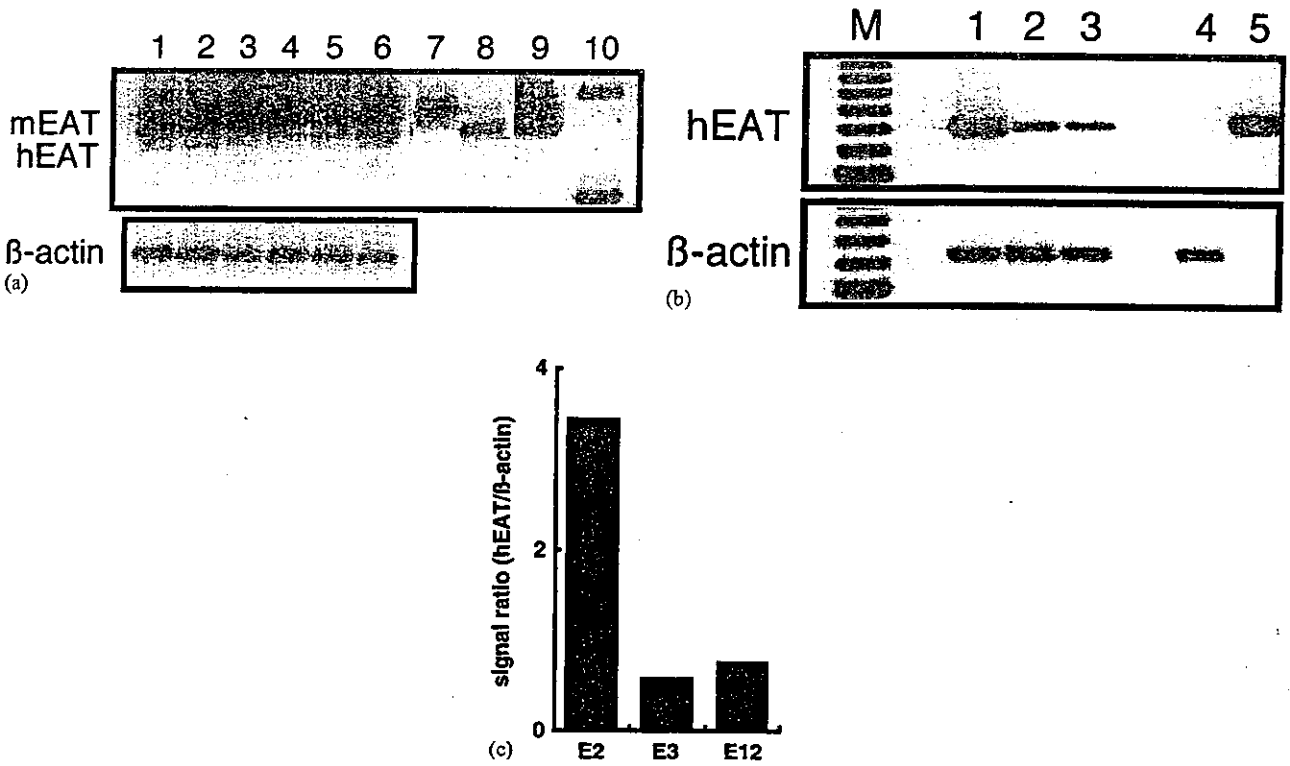

Fig. 2. Expression of the hEAT transgene by RT-PCR. Islet cells were isolated by collagenase treatment. (A) Expression of the hEAT transgene as assayed in various tissues compared with endogenous mEAT by RT-PCR. RT-PCR was performed with a primer set which detected both the hEAT transgene and endogenous mEAT but displayed two different bands (lane 1: liver; lane 2: kidney; lane 3: heart; lane 4: lung; lane 5: pituitary gland; lane 6: isolated islet cells from a E2 transgenic mouse). Controls included lane 7: liver from non-transgenic mouse (as a positive control for mEAT); lane 8: NCR-G3 cells, a human EC cell line (as a positive control for hEAT); and lane 9: a plasmid DNA mixture containing equal amounts of mouse and hEAT (as a quantitative control of the primer set). A 100 bp ladder is shown as a size marker in lane 10 (upper band: 400 bp; lower band: 300 bp). β-Actin (729 bp) RT-PCR products are shown to demonstrate the integrity of the isolated RNA (lower column). Langerhans islets (lane 6) exhibited higher expression levels of hEAT compared to other tissues. (B) Expression of the hEAT transgene in isolated islets from all three transgenic lines. RT-PCR was performed with a primer set which detected only the hEAT gene without detecting the endogenous mEAT gene (lane 1: E2; lane 2: E3; lane 3: E12; lane 4: non-transgenic mouse; lane 5: NCR-G3 cells). Islets from a non-transgenic mouse and NCR-G3 cells served as negative and positive controls, respectively. A 100 bp ladder is shown as a size marker in lane M. β-Actin (729 bp) RT-PCR products are shown to demonstrate the integrity of the isolated RNA (lower column). The β-actin band was not detected in human NCR-G3 cells (lane 5), since the primers were prepared specifically for the murine β-actin gene, and not for the human gene. (C) Bar graph representing the signal intensity ratio of hEAT to β-actin (hEAT/β-actin) for (B). A difference in hEAT expression can be detected in the three lines. The E2 line showed a higher expression level compared with the other two lines. The expression level in the E3 line was lowest; however, the difference between the E3 and E12 lines was subtle.

enlargement of islets was considered to be hyperplasia rather than adenoma. These hyperplastic islets in EAT transgenic mice develop between 4 and 24 months of age and were macroscopically visible in older animals.

For quantitative area measurements of the islet cell area, three lines of transgenic mice were used: E2, E3, and E12. Of the 29 transgenic mice studied, 7 were from the E12 line (ages ranging from 5 to 16 months), 10 were from the E2 line (ages ranging from 4 to 17.5 months), and 12 were from the E3 line (ages ranging from 7 to 14 months). Fourteen non-transgenic mice were studied (ages ranging from 4.5 to 14 months). Quantitative area measurement revealed the ratio of islet cell area to total pancreatic area in E2 or E12 transgenic mice to be higher than that in non-transgenic mice (Fig. 4). The ratio of islet cell area to total pancreatic area in E12 transgenic mice was significantly higher than that in non-transgenic mice ($P = 0.0021$). In contrast, the E3 transgenic mice did not show any increase in the islet cell area as compared to the non-transgenic mice.

3.4. Detection of other bcl-2 related genes in transgenic islet cells

We used the differential hybridization technique of Atlas™ Mouse cDNA expression array to identify genes which are differentially expressed either in EAT transgenic or non-transgenic islet cells. As shown in Fig. 5, Bax and Bag-1 were up-regulated in EAT transgenic islet cells compared with non-transgenic islet cells. Expression was not noted for Bcl-2, Bcl-xL, Bad, Bak, Bcl-w and Bid in either transgenic or non-transgenic islets. Selenoprotein, a glutathione peroxidase, and β-actin were used as internal controls and were expressed

(A)

(B)

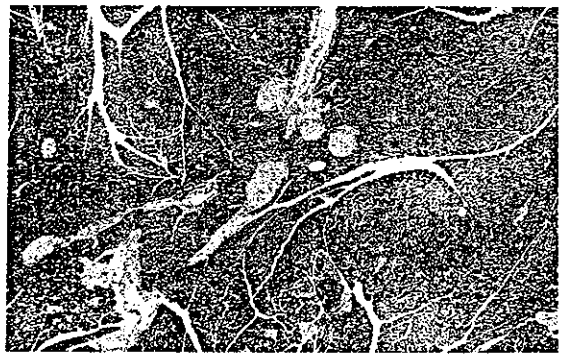

(C)

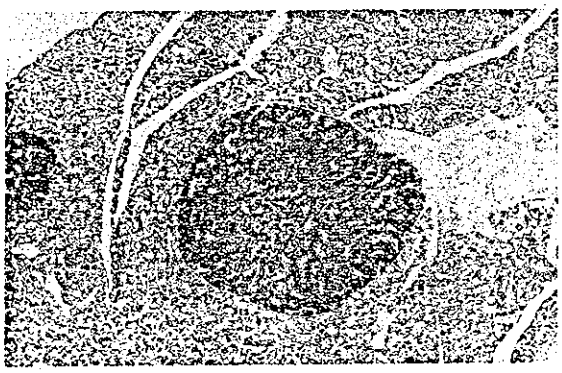

(D)

(E)

Fig. 3

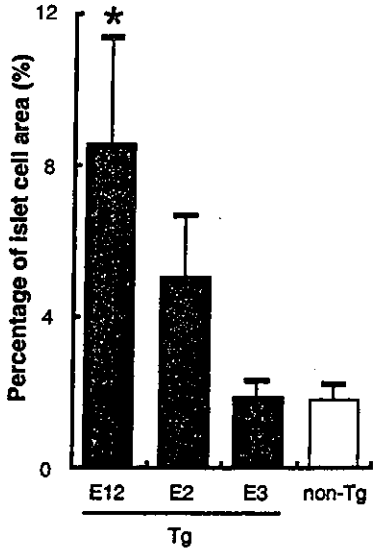

Fig. 4. Percentage of islet cell area to pancreas area. Three lines of transgenic mice were used: E2, E3, and E12. Of the 29 transgenic mice studied, 7 were from the E12 line (ages ranging from 5 to 16 months), 10 were from the E2 line (ages ranging from 4 to 17.5 months), and 12 were from the E3 line (ages ranging from 7 to 14 months). Fourteen non-transgenic mice were studied (ages ranging from 4.5 to 14 months). Each area was calculated from the H&E stained photos. Error bars represent SEM. Tg, transgenic mice; non-Tg, non-transgenic mice. $^*P < 0.05$ vs non-Tg.

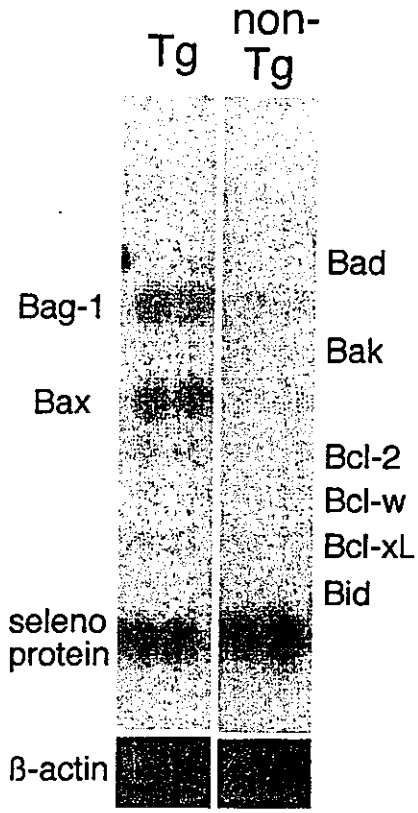

Fig. 5. Differential hybridization of cDNA expression arrays of isolated islets. The expression of bcl-2 related genes in transgenic islets was compared to expression in non-transgenic islets. The left and right panels represent expression array membranes hybridized with cDNA from transgenic and non-transgenic islets, respectively. Bax and Bag-1 were up-regulated in EAT transgenic islets compared with non-transgenic islets. Expression was not noted for Bcl-2, Bcl-xL, Bad, Bak, Bcl-w and Bid in either transgenic or non-transgenic islets. Selenoprotein, a glutathione peroxidase, and β-actin were used as internal controls and were expressed at similar levels in both EAT transgenic and non-transgenic mouse. Tg, transgenic mice; non-Tg, non-transgenic mice.

at similar levels in both EAT transgenic and non-transgenic mouse. These findings suggest that EAT participates in the control of apoptosis in islet cells.

3.5. Insulin secretion in the hyperplastic islets

We next measured serum insulin levels by ELISA to test the insulin secretion ability of these hyperplastic islets. Serum insulin levels were measured 15 min after intraperitoneal glucose administration following overnight fasting. As shown in Fig. 6A, a trend towards higher serum insulin levels was observed in the EAT transgenic mice; however, this difference was not statistically significant.

Fatty metamorphosis of the liver was observed in EAT transgenic mice which exhibited exceedingly high levels of serum insulin (Fig. 7). A trend towards lower blood glucose levels was observed in the transgenic mice which produced these high serum insulin levels; however, this difference was not as marked as the difference in serum insulin levels between transgenic and non-transgenic animals (data not shown).

We also assessed insulin sensitivity by an i.p. insulin tolerance test. The insulin tolerance test on E12 mice showed no significant difference in the hypoglycemic response to insulin between transgenic and non-transgenic mice (Fig. 6B). We therefore concluded that the changes we observed in islet size were not due to insulin resistance.

Fig. 3. Islet cell hyperplasia in transgenic mice overexpressing EAT. (A) Macroscopic findings of islet cell hyperplasia in an EAT transgenic mouse. Many large tumors were observed in the pancreas (as indicated by arrowheads). This photo shows the pancreas from a 8-month-old mouse from the E2 line. (B) Hyperplasia of the islets of Langerhans in the EAT transgenic mice. This specimen was prepared from a 16-month-old mouse from the E12 line. H&E staining. Original magnifications, × 20. (C) Normal appearance of islets in a 12-month-old non-transgenic mouse from the E12 line. H&E staining. Original magnifications, × 20. (D–E) Immunohistochemical analysis for insulin (D) and glucagon (E). Specimens were prepared from a 16-month-old EAT transgenic mouse from the E12 line. The majority of the enlarged Langerhans islets were positive for insulin while cells positive for glucagon were observed only sporadically. Thus, the enlargement of islets was considered to be hyperplasia. Original magnifications, × 40.

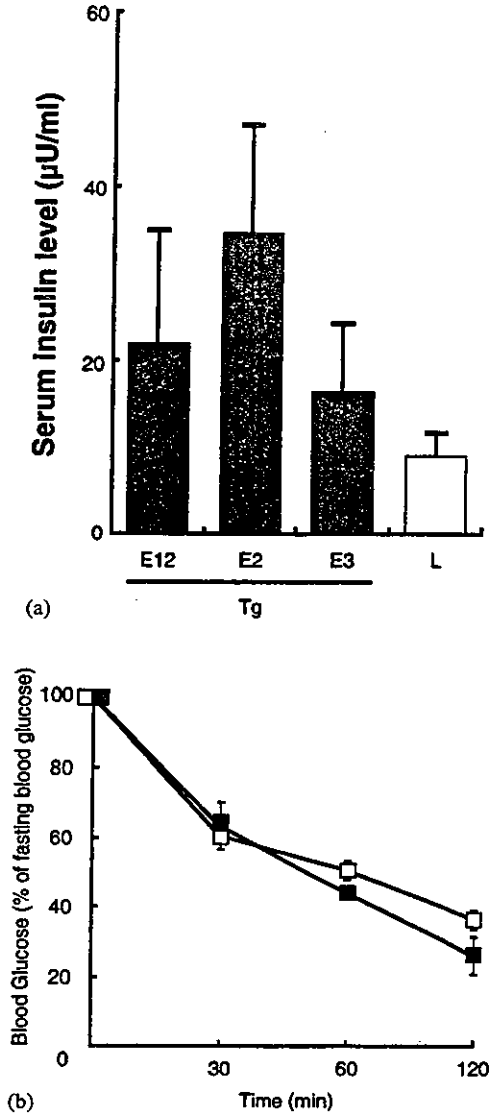

Fig. 6. Serum insulin levels and insulin tolerance test. (A) Measurement of insulin in EAT transgenic mice and non-transgenic mice. Three lines of transgenic mice were used for analysis. Of the 24 transgenic mice studied, 13 were from the E12 line (ages ranging from 8 to 22 months), 3 were from the E2 line (ages ranging from 19 to 24 months), and 8 were from the E3 line (ages ranging from 8 to 19 months). Thirty-three non-transgenic mice were studied (age 8 months). Mice were fasted overnight prior to intraperitoneal glucose administration (2 mg glucose/g BW). Blood was collected from the right cardiac ventricle 15 min after glucose administration. Error bars represent SEM. Tg, transgenic mice; non-Tg, non-transgenic mice. (B) Insulin tolerance test in EAT transgenic (open square) and non-transgenic (closed square) mice. Of the 8 mice from the E12 line studied, 4 were transgenic (age 8 months) and 4 were non-transgenic (ages ranging from 5 to 8 months). After overnight fasting, insulin (0.5 Units/kg BW) was injected into the peritoneal cavity of mice. Blood samples were collected from the tail at the indicated time and glucose concentrations were measured. Error bars represent SEM.

3.6. Islet cell adenoma in the EAT transgenic mouse

In addition to the above hyperplastic changes, we observed an extremely enlarged islet juxtaposed to hyperplastic islets in one EAT transgenic mouse (Fig. 8A). Histological analysis of this region revealed a coarse chromatin structure of the nuclei and prominent nucleoli compared with normal islets (Fig. 8B and C). In this enlarged islet region, all the cells were positive for insulin and there were no cells positive for glucagon (data not shown). Thus, this enlarged islet was considered to be an adenoma rather than a hyperplasia. This islet cell adenoma may have developed because of a second hit or mutation to certain genes governing the malignant transformation of cells.

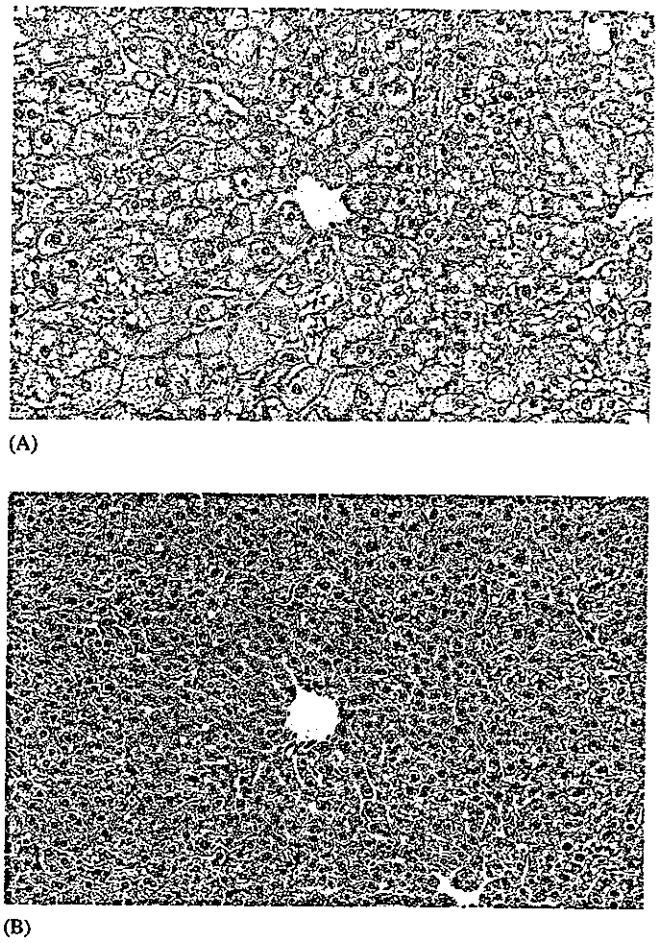

Fig. 7. Fatty metamorphosis of the liver in EAT transgenic mice. (A) Severe fatty metamorphosis was observed in the liver of transgenic mice in association with islet cell hyperplasia. (B) Normal appearance of hepatocytes in the non-transgenic liver. H&E staining. Original magnifications, × 100.

4. Discussion

4.1. Mechanisms of islet cell hyperplasia in EAT transgenic mice

Apoptosis plays a key role in normal development and tissue homeostasis (Korsmeyer, 1995; Lewin and

(A)

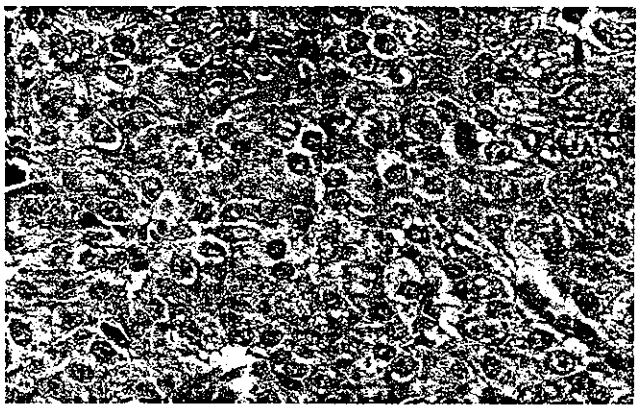

(B)

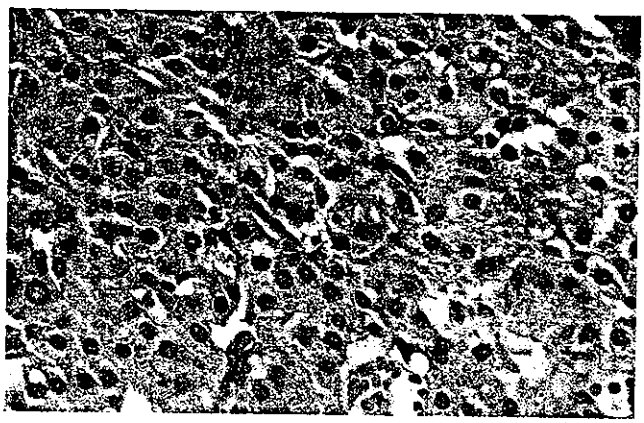

(C)

Fig. 8

Barde, 1996). β cells in the adult endocrine pancreas have been reported to have a life span of approximately 30 days, after which they undergo apoptosis (Finegood et al., 1995). The process of replication and proliferation in the pancreas—the neogenesis of new β cells derived from progenitor cells that bud from the ducts of the exocrine pancreas—allows for the replacement of these apoptotic β cells. Mathematical models have shown that though the replication rate of β cells in the adult rodent is only about 3% per day, the β-cell mass will double in 1 month if the apoptotic elimination of β cells are ignored (Finegood et al., 1995).

The EAT gene is considered to be a member of the bcl-2 related gene family based upon its possession of the BH domains 1, 2, 3 and 4 (Kroemer, 1997; Revilla et al., 1997). Similar to bcl-2, EAT has been shown to inhibit apoptosis in vitro (Reynolds et al., 1994; Sano et al., 2001). BH domains (BH1 to BH4) determine the capacity of bcl-2 related proteins to interact with each other or with other unrelated proteins. The ratio of death antagonists to agonists is known to determine whether a cell will undergo apoptosis. This death-life balance is regulated partly by competitive dimerization between pairs of antagonists and agonists (Kroemer, 1997). Up-regulation of Bax and Bag-1, both bcl-2 related genes, in EAT transgenic islets supports the hypothesis that EAT could inhibit apoptosis of pancreatic islet cells. Bax, which is known to be a pro-apoptotic molecule and heterodimeric partner for Bcl-2, was reported to display the same pattern of combinatorial interactions with EAT as Bcl-2 (Sedlak et al., 1995; Yang et al., 1995b). Similar to bcl-2, EAT may heterodimerize with Bax through BH1 and BH2 domains to repress apoptosis. Bag-1, an anti-apoptotic molecule, can interact with Bcl-2 and coexpression of BCL-2 and BAG-1 is more protective than expression of either protein alone (Schulz et al., 1997; Terada et al., 1997). Although Bag-1 has not been demonstrated to combine with EAT, Bag-1 may be a possible heterodimeric partner for EAT as it docks to the BH4 domain which EAT has been shown to possess (Kroemer, 1997).

The human bcl-2 gene has been shown to prevent cytokine-induced β-cell apoptosis in pancreatic islet cells (Iwahashi et al., 1996; Liu et al., 1996). Our results suggests that the protection afforded by EAT towards

Fig. 8. Islet cell adenoma in one EAT transgenic mouse. (A) An islet-cell adenoma was observed in one 16-month-old EAT transgenic mouse from the E12 line. H&E staining. Original magnifications, × 10. (B) Atypical nuclei are observed in the adenoma cells. Prominent nucleoli and a coarse chromatin pattern are observed in the adenoma cells. H&E staining. Original magnifications, × 400. (C) Normal appearance of pancreatic islet cells in a 12-month-old non-transgenic mouse from the E12 line. H&E staining. Original magnifications, × 400.

islet cell apoptosis led to islet cell hyperplasia in these transgenic mice.

4.2. Hyperplasia is observed with only the islets of the pancreas and is detected only after 4 months of age

The use of the EF1α promoter allows for ubiquitous tissue expression of the EAT transgene, yet hyperplastic changes were observed in only the pancreatic islets and not in other tissues. One possible mechanism may be that the expression level of the transgene was higher in pancreatic islets compared with other tissues. Another possible factor may be the lack of expression of genes which could block EAT function in the pancreatic islets. No bcl-2 related genes were detected in non-transgenic islets. Thus we would like to hypothesize that molecules which could block EAT function in the apoptotic pathway may not be expressed in the pancreatic islets and allow for this exaggerated effect of EAT in islet cells. In other words, the cellular environment in pancreatic islets may be suited for this EAT-induced hyperplasia (Cheatham and Kahn, 1995; Saltiel, 1996).

Hyperplasia was not observed in EAT transgenic mice before the age of 4 months. This may be due to the dynamics of islet cell growth based on the process of cell proliferation and apoptosis. During the neonatal period, approximately 10% of the fetal islet cells are undergoing apoptosis at any given point, but this fraction decreases to 3% in adult islets indicating that cell replication decreases after the neonatal period (Finegood et al., 1995). The fraction of apoptotic cells remains almost constant after the neonatal period. This ratio of cell proliferation to apoptosis is a critical determinant of total islet cell mass; while total islet cell and pancreatic mass increases dramatically due to the high proliferation rate before 4 months of age, the total mass maintains a stable balance after 4 months of age due to the relative decrease in this ratio of cell proliferation to apoptosis. Therefore, the influence of apoptosis on islet cell mass remains negligible before 4 months of age, but becomes a more significant factor after 4 months of age.

4.3. Differences among three transgenic lines

A difference in the incidence of islet cell hyperplasia was observed among the three transgenic lines. Fewer hyperplastic islets were observed in the E3 line as compared to the other two lines. This finding may suggest that the E3 line does not show any specific phenotype. This may be explained by three factors: expression level, copy number, and integration site. The phenotypes that we observed in the various lines were closely correlated with expression levels. The expression level of hEAT was found to be highest in the E2 line and to be lowest in the E3 line, though the difference between the E3 and E12 lines was subtle. In contrast, we found that the copy number of the transgene per diploid genome in the E3 line was higher compared with the other two lines; however, it is known that expression level is independent of copy number. We were not able to correlate our phenotypes with the integration sites, and find it difficult to forward a precise explanation for this; nevertheless, gene induction is known to be stochastic (Ko, 1992; Ko et al., 1990b) and variability of results is commonly observed with the transgenic approach.

4.4. Clinical impact of the anti-apoptotic activities of EAT in β cells

Our results suggest that EAT may play a role in the inhibition of pancreatic β cells from apoptosis in vivo. Apoptosis of β cells is considered to be a prevalent mechanism in insulin-dependent diabetes mellitus (IDDM) (Rossini et al., 1993), a T-cell mediated autoimmune disease (McInerney et al., 1996; Wong and Janeway, 1997). Although the precise role of apoptosis in β cell destruction in IDDM remains to be defined, both soluble mediators and Fas antigen may possibly be involved (Chervonsky et al., 1997; Itoh et al., 1993). Cytotoxic T cells can induce apoptosis of β cells via the Fas pathway, and overexpression of bcl-2 has been reported to inhibit this Fas-induced cell death (Itoh et al., 1993). The possession of anti-apoptotic activity by EAT towards β cells, shown in this investigation, suggests the use of EAT under certain conditions to inhibit or delay apoptosis of β cells. Establishment of EAT inhibition of β cell apoptosis in humans, hints at possible future genetic therapies for IDDM.

Acknowledgements

We are grateful to J. Ozawa, K. Otsuki, H. Suzuki, S. Kusakari, H. Abe, Y. Hashimoto and M. Takahashi for their technical assistance and K. Takeichi for photographic assistance. We also thank to T. Ando, H. Kikuchi, T. Atsumi, and A. Hashiguchi for useful discussion. This work was supported in part by a grant from the Ministry of Education, Science and Culture to J.H. and A.U., by Keio University Special Grant-in-Aid for Innovative Collaborative Research Project to J.H. and A.U., by Keio Gijuku Fukuzawa Memorial Funds for the Advancement of Education and Research from Keio University to H.O., and by a National Grant-in-Aid for the Establishment of a High-Tech Research Center at Private Universities.

References

Adams, J.M., Cory, S., 1998. The Bcl-2 protein family: arbiters of cell survival. Science 281, 1322–1326.

Akgul, C., Moulding, D.A., White, M.R., Edwards, S.W., 2000a. In vivo localisation and stability of human Mcl-1 using green fluorescent protein (GFP) fusion proteins. FEBS Lett. 478, 72–76.

Akgul, C., Turner, P.C., White, M.R., Edwards, S.W., 2000b. Functional analysis of the human MCL-1 gene. Cell Mol. Life Sci. 57, 684–691.

Ando, T., Umezawa, A., Suzuki, A., Okita, H., Sano, M., Hiraoka, Y., Aiso, S., Saruta, T., Hata, J., 1998. EAT/mcl-1, a member of the bcl-2 related genes, confers resistance to apoptosis induced by cis-diammine dichloroplatinum (II) via a p53- independent pathway. Jpn J. Cancer Res. 89, 1326–1333.

Bingle, C.D., Craig, R.W., Swales, B.M., Singleton, V., Zhou, P., Whyte, M.K., 2000. Exon skipping in Mcl-1 results in a bcl-2 homology domain 3 only gene product that promotes cell death. J. Biol. Chem. 275, 22136–22146.

Boise, L.H., Gonzalez-Garcia, M., Postema, C.E., Ding, L., Lindsten, T., Turka, L.A., Mao, X., Nunez, G., Thompson, C.B., 1993. bcl-x, a bcl-2-related gene that functions as a dominant regulator of apoptotic cell death. Cell 74, 597–608.

Brady, H.J., Gil-Gomez, G., Kirberg, J., Berns, A.J., 1996a. Bax alpha perturbs T cell development and affects cell cycle entry of T cells. EMBO J. 15, 6991–7001.

Brady, H.J., Salomons, G.S., Bobeldijk, R.C., Berns, A.J., 1996b. T cells from baxalpha transgenic mice show accelerated apoptosis in response to stimuli but do not show restored DNA damage-induced cell death in the absence of p53 gene product in. EMBO J. 15, 1221–1230.

Chao, D.T., Korsmeyer, S.J., 1998. BCL-2 family: regulators of cell death. Annu. Rev. Immunol. 16, 395–419.

Cheatham, B., Kahn, C.R., 1995. Insulin action and the insulin signaling network. Endocr. Rev. 16, 117–142.

Chervonsky, A.V., Wang, Y., Wong, F.S., Visintin, I., Flavell, R.A., Janeway, C., Jr., Matis, L.A., 1997. The role of Fas in autoimmune diabetes. Cell 89, 17–24.

Chittenden, T., Harrington, E.A., O'Connor, R., Flemington, C., Lutz, R.J., Evan, G.I., Guild, B.C., 1995. Induction of apoptosis by the Bcl-2 homologue Bak. Nature 374, 733–736.

D'Sa-Eipper, C., Subramanian, T., Chinnadurai, G., 1996. bfl-1, a bcl-2 homologue, suppresses p53-induced apoptosis and exhibits potent cooperative transforming activity. Cancer Res. 56, 3879–3882.

Finegood, D.T., Scaglia, L., Bonner-Weir, S., 1995. Dynamics of beta-cell mass in the growing rat pancreas. Estimation with a simple mathematical model. Diabetes 44, 249–256.

Gibson, L., Holmgreen, S.P., Huang, D.C., Bernard, O., Copeland, N.G., Jenkins, N.A., Sutherland, G.R., Baker, E., Adams, J.M., Cory, S., 1996. bcl-w, a novel member of the bcl-2 family, promotes cell survival. Oncogene 13, 665–675.

Gotoh, M., Maki, T., Kiyoizumi, T., Satomi, S., Monaco, A.P., 1985. An improved method for isolation of mouse pancreatic islets. Transplantation 40, 437–438.

Hanaoka, K., Hayasaka, M., Uetsuki, T., Fujisawa-Sehara, A., Nabeshima, Y., 1991. A stable cellular marker for the analysis of mouse chimeras: the bacterial chloramphenichol acetyltransferase driven by the human elongation factor 1a promoter. Differentiation 48, 183–189.

Hata, J.-I., Fujimoto, J., Ishii, E., Umezawa, A., Kokai, Y., Matsubayashi, Y., Abe, H., Kusakari, S., Kikuchi, H., Yamada, T., Maruyama, T., 1992. Differentiation of human germ cell tumor cells in vivo and in vitro. Acta Histochem. Cyotchem. 25, 563–576.

Hogan, B., Constantini, F., Howard, B.H., 1986. Manipulating The Mouse Embryo. Cold Spring Harbor Laboratory Press, New York.

Inohara, N., Ding, L., Chen, S., Nunez, G., 1997. Harakiri, a novel regulator of cell death, encodes a protein that activates apoptosis and interacts selectively with survival-promoting proteins Bcl-2 and Bcl-X(L). EMBO J. 16, 1686–1694.

Itoh, N., Tsujimoto, Y., Nagata, S., 1993. Effect of bcl-2 on Fas antigen-mediated cell death. J. Immunol. 151, 621–627.

Iwahashi, H., Hanafusa, T., Eguchi, Y., Nakajima, H., Miyagawa, J., Itoh, N., Tomita, K., Namba, M., Kuwajima, M., Noguchi, T., Tsujimoto, Y., Matsuzawa, Y., 1996. Cytokine-induced apoptotic cell death in a mouse pancreatic beta-cell line: inhibition by Bcl-2. Diabetologia 39, 530–536.

Knudson, C.M., Tung, K.S., Tourtellotte, W.G., Brown, G.A., Korsmeyer, S.J., 1995. Bax-deficient mice with lymphoid hyperplasia and male germ cell death. Science 270, 96–99.

Ko, M.S., 1992. Induction mechanism of a single gene molecule: stochastic or deterministic? Bioessays 14, 341–346.

Ko, M.S., Ko, S.B., Takahashi, N., Nishiguchi, K., Abe, K., 1990a. Unbiased amplification of a highly complex mixture of DNA fragments by 'lone linker'-tagged PCR. Nucleic Acids Res. 18, 4293–4294.

Ko, M.S., Nakauchi, H., Takahashi, N., 1990b. The dose dependence of glucocorticoid-inducible gene expression results from changes in the number of transcriptionally active templates. EMBO J. 9, 2835–2842.

Korsmeyer, S.J., 1995. Regulators of cell death. Trends. Genet. 11, 101–105.

Kozopas, K.M., Yang, T., Buchan, H.L., Zhou, P., Craig, R.W., 1993. MCL1, a gene expressed in programmed myeloid cell differentiation, has sequence similarity to BCL2. Proc. Natl. Acad. Sci. USA 90, 3516–3520.

Kroemer, G., 1997. The proto-oncogene Bcl-2 and its role in regulating apoptosis. Nat. Med. 3, 614–620.

Lacy, P.E., Kostianovsky, M., 1967. Method for the isolation of intact islets of Langerhans from the rat pancreas. Diabetes 16, 35–39.

Lewin, G.R., Barde, Y.A., 1996. Physiology of the neurotrophins. Annu. Rev. Neurosci. 19, 289–317.

Lin, E.Y., Orlofsky, A., Wang, H.G., Reed, J.C., Prystowsky, M.B., 1996. A1, a Bcl-2 family member, prolongs cell survival and permits myeloid differentiation. Blood 87, 983–992.

Liu, Y., Rabinovitch, A., Suarez-Pinzon, W., Muhkerjee, B., Brownlee, M., Edelstein, D., Federoff, H.J., 1996. Expression of the bcl-2 gene from a defective HSV-1 amplicon vector protects pancreatic beta-cells from apoptosis. Hum. Gene Ther. 7, 1719–1726.

Matsushita, K., Umezawa, A., Iwanaga, S., Oda, T., Okita, H., Kimura, K., Shimada, M., Tanaka, M., Sano, M., Ogawa, S., Hata, J., 1999. The EAT/mcl-1 gene, an inhibitor of apoptosis, is up-regulated in the early stage of acute myocardial infarction. Biochim. Biophys. Acta 1472, 471–478.

McDonnell, T.J., Deane, N., Platt, F.M., Nunez, G., Jaeger, U., McKearn, J.P., Korsmeyer, S.J., 1989. bcl-2-immunoglobulin transgenic mice demonstrate extended B cell survival and follicular lymphoproliferation. Cell 57, 79–88.

McInerney, M.F., Flynn, J.C., Goldblatt, P.J., Najjar, S.M., Sherwin, R.S., Janeway, C., Jr., 1996. High density insulin receptor-positive T lymphocytes from nonobese diabetic mice transfer insulitis and diabetes. J. Immunol. 157, 3716–3726.

Moulding, D.A., Giles, R.V., Spiller, D.G., White, M.R., Tidd, D.M., Edwards, S.W., 2000. Apoptosis is rapidly triggered by antisense depletion of MCL-1 in differentiating U937 cells. Blood 96, 1756–1763.

Okita, H., Umezawa, A., Suzuki, A., Hata, J., 1998. Up-regulated expression of murine Mcl1/EAT, a bcl-2 related gene, in the early stage of differentiation of murine embryonal carcinoma cells and embryonic stem cells. Biochim. Biophys. Acta 1398, 335–341.

Reed, J.C., 1998. Bcl-2 family proteins. Oncogene 17, 3225–3236.

Revilla, Y., Cebrian, A., Baixeras, E., Martinez, C., Vinuela, E., Salas, M.L., 1997. Inhibition of apoptosis by the African swine fever

virus Bcl-2 homologue: role of the BH1 domain. Virology 228, 400–404.

Reynolds, J.E., Yang, T., Qian, L., Jenkinson, J.D., Zhou, P., Eastman, A., Craig, R.W., 1994. Mcl-1, a member of the Bcl-2 family, delays apoptosis induced by c-Myc overexpression in Chinese hamster ovary cells. Cancer Res. 54, 6348–6352.

Rossini, A.A., Greiner, D.L., Friedman, H.P., Mordes, J.P., 1993. Immunopathogenesis of diabetes mellitus. Diabetes Rev. 1, 43–75.

Saltiel, A.R., 1996. Diverse signaling pathways in the cellular actions of insulin. Am. J. Physiol. 270, E375–E385.

Sano, M., Umezawa, A., Abe, H., Akatsuka, A., Nonaka, S., Shimizu, H., Fukuma, M., Hata, J., 2001. EAT/mcl-1 expression in the human embryonal carcinoma cells undergoing differentiation or apoptosis. Exp. Cell Res. 266, 114–125.

Sano, M., Umezawa, A., Suzuki, A., Shimoda, K., Fukuma, M., Hata, J., 2000. Involvement of EAT/mcl-1, an anti-apoptotic bcl-2-related gene, in murine embryogenesis and human development. Exp. Cell Res. 259, 127–139.

Schulz, J.B., Bremen, D., Reed, J.C., Lommatzsch, J., Takayama, S., Wullner, U., Loschmann, P.A., Klockgether, T., Weller, M., 1997. Cooperative interception of neuronal apoptosis by BCL-2 and BAG-1 expression: prevention of caspase activation and reduced production of reactive oxygen species. J. Neurochem. 69, 2075–2086.

Sedlak, T.W., Oltvai, Z.N., Yang, E., Wang, K., Boise, L.H., Thompson, C.B., Korsmeyer, S.J., 1995. Multiple Bcl-2 family members demonstrate selective dimerizations with Bax. Proc. Natl. Acad. Sci. USA 92, 7834–7838.

Sentman, C.L., Shutter, J.R., Hockenbery, D., Kanagawa, O., Korsmeyer, S.J., 1991. bcl-2 inhibits multiple forms of apoptosis but not negative selection in thymocytes. Cell 67, 879–888.

Siegel, R.M., Katsumata, M., Miyashita, T., Louie, D.C., Greene, M.I., Reed, J.C., 1992. Inhibition of thymocyte apoptosis and negative antigenic selection in bcl-2 transgenic mice. Proc. Natl. Acad. Sci. USA 89, 7003–7007.

Strasser, A., Harris, A.W., Cory, S., 1991. bcl-2 transgene inhibits T cell death and perturbs thymic self-censorship. Cell 67, 889–899.

Terada, S., Fukuoka, K., Fujita, T., Komatsu, T., Takayama, S., Reed, J.C., Suzuki, E., 1997. Anti-apoptotic genes, bag-1 and bcl-2, enabled hybridoma cells to survive under treatment for arresting cell cycle. Cytotechnology 25, 17–23.

Umezawa, A., Maruyama, T., Inazawa, J., Imai, S., Takano, T., Hata, J., 1996. Induction of mcl1/EAT, Bcl-2 related gene, by retinoic acid or heat shock in the human embryonal carcinoma cells, NCR-G3. Cell Struct. Funct. 21, 143–150.

Veis, D.J., Sorenson, C.M., Shutter, J.R., Korsmeyer, S.J., 1993. Bcl-2-deficient mice demonstrate fulminant lymphoid apoptosis, polycystic kidneys, and hypopigmented hair. Cell 75, 229–240.

Wang, K., Yin, X.M., Chao, D.T., Milliman, C.L., Korsmeyer, S.J., 1996. BID: a novel BH3 domain-only death agonist. Genes Dev. 10, 2859–2869.

Wong, F.S., Janeway, C., Jr., 1997. The role of CD4 and CD8 T cells in type I diabetes in the NOD mouse. Res. Immunol. 148, 327–332.

Yang, E., Zha, J., Jockel, J., Boise, L.H., Thompson, C.B., Korsmeyer, S.J., 1995a. Bad, a heterodimeric partner for Bcl-XL and Bcl-2, displaces Bax and promotes cell death. Cell 80, 285–291.

Yang, T., Kozopas, K.M., Craig, R.W., 1995b. The intracellular distribution and pattern of expression of Mcl-1 overlap with, but are not identical to, those of Bcl-2. J. Cell Biol. 128, 1173–1184.

J Periodont Res 2003; 38; 333–342
Printed in the UK. All rights reserved

JOURNAL OF PERIODONTAL RESEARCH
ISSN 0022-3484

The effects of enamel matrix derivative (EMD) on osteoblastic cells in culture and bone regeneration in a rat skull defect

Satoshi Yoneda[1], Daisuke Itoh[1], Shinji Kuroda[1], Hisatomo Kondo[1], Akihiro Umezawa[2], Keiichi Ohya[3], Takashi Ohyama[4], Shohei Kasugai[1]

[1]Masticatory Function Control, Tokyo Medical and Dental University, [2]Pathology, Keio University School of Medicine, [3]Pharmacology, Hard Tissue Engineering, Tokyo Medical and Dental University, [4]Removable Prosthodontics, Tokyo Medical and Dental University, Tokyo, Japan

Yoneda S, Itoh D, Kuroda S, Kondo H, Umezawa A, Ohya K, Ohyama T, Kasugai S. The effects of enamel matrix derivative (EMD) on osteoblastic cells in culture and bone regeneration in a rat skull defect. J Periodont Res 2003; 38; 333–342. © Blackwell Munksgaard, 2003

Objective: Enamel matrix derivative (EMD) has been clinically used to promote periodontal tissue regeneration. The purpose of the present study is to clarify EMD affects on osteoblastic cells and bone regeneration.

Materials and Methods: Mouse osteoblastic cells (ST2 cells and KUSA/A1 cells) are used in culture experiments. After cells were treated with EMD, cell growth was evaluated with DNA measurement, 5-bromo-2′-deoxyurydine (BrdU) incorporation assay. Measurement of alkaline phosphatase (ALP) activity and mineralized-nodule (MN) formation, Northern blotting analysis and zymography are also performed. In addition, EMD was applied to a rat skull defect and the defect was radiographically and histologically evaluated 2 weeks after the application.

Results: EMD did not stimulate ST2 cell growth; however, it enhanced KUSA/A1 cell proliferation. Although EMD stimulated ALP activity in both the cells, ALP activity in KUSA/A1 cells was affected to a much greater degree. Corresponding to the increase in ALP activity, MN formation in KUSA/A1 cells was enhanced by EMD. EMD stimulated osteoblastic phenotype expression of KUSA/A1 cells such as type I collagen, osteopontin, transforming growth factor beta 1 and osteocalcin. EMD treatment also stimulated matrix metalloproteinase production in KUSA/A1 cells. Although the effects of EMD on osteoblastic cells depend on cell type, the overall effect of EMD on osteoblastic cells is stimulatory rather than inhibitory. Finally, EMD application to a rat skull defect accelerated new bone formation.

Conclusion: These results indicate that EMD affects osteoblastic cells and has potential as a therapeutic material for bone healing.

Satoshi Yoneda, DDS, Masticatory Function Control, Tokyo Medical and Dental University, 1-5-45, Yushima, Bunkyo-ku, Tokyo, 113-8549, Japan
Tel: +81 3 5803 4554
Fax: +81 3 5803 5934
e-mail: kome.mfc@tmd.ac.jp

Key words: enamel matrix derivative; osteoblasts; culture; skull defect

Accepted for publication October 28, 2002

The implication of enamel matrix in cementogenesis in tooth development was suggested more than 20 years ago (1). In 1997, Hammarström (2) reported the formation of acellular cementum after experimentally exposing dental follicles [the progenitors of cementum, periodontal ligament (PDL) and alveolar bone] to enamel matrix. Furthermore, he and his collaborators (3, 4) demonstrated that enamel matrix derivative induces the formation of acellular cementum on denuded root surfaces in monkeys and humans. Thus, it is a logical choice to use enamel matrix derivative for periodontal tissue regeneration. EMD, in acid-extracted porcine

enamel derivative form, is commercially available.

Animal experiments (5–7) and clinical studies (8–12) have already demonstrated that EMD stimulates regeneration of periodontal tissue, including acellular cementum, PDL and alveolar bone. The effects of EMD on PDL cells in culture have been examined. EMD stimulates cellular proliferation, migration, alkaline phosphatase (ALP) activity, mineralized nodule (MN) formation, and transforming growth factor beta 1 (TGF-β1) production (13–15). These EMD effects on PDL cells could favorably contribute to periodontal tissue regeneration.

It has been reported that EMD affects osteoblastic cells *in vitro* (16, 17), and its effects depend on cell type; however, the precise effect of EMD on osteoblastic cells needs to be elucidated. In the present study, we used two mouse osteoblastic cell lines, ST2 and KUSA/A1 cells. ST2 cells can differentiate to the adipocyte and osteoblast. Although their osteoblastic differentiation and maturation are induced and stimulated by ascorbic acid, osteoblastic differentiation of ST2 cells needs a long period (18). On the other hand, KUSA/A1 cells have the ability to differentiate to osteoblast and they can form bone-like tissue early both *in vitro* and *in vivo* (19). Compared with ST2 cells, KUSA/A1 cells are highly committed to osteoblastic linage. To examine the effect of EMD on the osteoblastic differentiation and maturation, the following analyses were performed *in vitro*: cellular proliferation, ALP activity, MN formation, matrix metalloproteinase (MMP) production and mRNA expression of osteoblastic phenotypes.

The effect of EMD on bone *in vivo* has been reported: EMD enhances bone formation induced by bone morphogenetic protein (BMP) (20) and it stimulates bone regeneration of rat femurs (21). BMP-induced bone formation usually follows endochondral ossification and it is unlikely that bone regeneration of femur is similar to the one of oral-maxillofacial bones. Thus, in the present study, we used calvarial bone defect model to evaluate EMD effect on bone regeneration.

Materials and methods

EMD treatment and cell culture

EMD (Biora, Malmö, Sweden) was dissolved in 10 mM acetic acid and stored at −70°C. Before cell inoculation, a serum-free culture medium was added to the culture plates. Various concentrations of EMD (from 12.5 to 50 μg/ml) were added and the culture plates were incubated in a CO_2 incubator for 3 h. EMD precipitated and a fine deposition of EMD covered the bottom of the plates. This treatment did not affect the medium's pH. Two mouse osteoblastic cell lines, ST2 cells and KUSA/A1 cells, were used. ST2 cells were purchased from RIKEN Cell Bank (Saitama, Japan); KUSA/A1 cells were established by Umezawa (19), one of the authors. These cells were suspended in medium containing 20% FBS, and then inoculated onto plates that contained serum-free medium with EMD. The final concentration of FBS in the medium was 10%. After 24 h, the medium was aspirated without removing the precipitated EMD, and new culture medium was added to the plates. In all the experiments except the proliferation assays and ALP activity measurement, the culture medium was α-MEM (minimum essential medium alpha medium, GIBCO, Tulsa, OK, USA) supplemented with 10% fetal bovine serum (FBS: Lot no. 6H2167, Summit, Collins, CO, USA), 60 μg/ml kanamycin and 0.2 mM L-ascorbic acid phosphate magnesium salt (Wako Chemical Co., Osaka, Japan). The culture medium for KUSA/A1 cells was additionally supplemented with 5 mM β-glycerophosphate disodium salt (Sigma Chemical Co., St. Louis, MO, USA). The culture was maintained at 37°C in a humidified atmosphere consisting of 95% air and 5% CO_2.

Proliferation assays (DNA measurement and BrdU incorporation)

In proliferation assay experiments, FBS concentration in the culture medium was 5%. Ninety-six-well plates and 24-well plates were treated with EMD as described above. For DNA measurement, ST2 cells and KUSA/A1 cells were inoculated in 24-well plates at a cell density of 10^4 cells/cm^2 and 10^3 cells/cm^2, respectively. ST2 cells and KUSA/A1 cells were rinsed with Ca^{2+}-, Mg^{2+}-free phosphate buffered saline [PBS (−)], scraped into 0.3 ml of 0.9% NaCl containing 0.1% sodium dodecyl sulfate (SDS), and then homogenized using a sonicator (Sonicator 5202, Otake, Japan) on ice after 10 and 16 d, respectively. DNA content was spectrofluorometrically determined by the method reported by Labarca (22). Fifty microliters of the sample was mixed with Hoechst 33258 buffer (1 μg/ml Hoechst 33258, 0.05 M Na_3PO_4, 2.0 M NaCl, and 2.0 mM EDTA, pH 7.4). The fluorescence was read at 356 nm excitation and 458 nm emission using a spectrofluorometer (FP-777, JASCO, Japan). Salmon sperm DNA was used as the standard.

For the 5-bromo-2′-deoxyuridine (BrdU) incorporation assay, KUSA/A1 cells were inoculated into 96-well plates at a cell density of 10^3 cells/cm^2 and cultured. A BrdU incorporation assay (Amersham Pharmacia Biotech, UK) was performed at d 4, 8 and 14, following the manufacturer's instructions. In brief, the cells were labeled with BrdU for 24 h. The pyrimidine analogue BrdU was incorporated instead of thymidine into the DNA of proliferating cells (23) and incorporated BrdU was detected by means of enzyme-linked immunosorbent assay. The absorbance of resultant color was read at 450 nm in a microtitre plate spectrophotometer (Microplate Reader, Model 450, Bio-Rad).

Measurement of ALP activity

The activity of ALP was measured in both ST2 and KUSA/A1 cells. The sample was the same as the one used for DNA measurement and prepared as described above. In the culture of ST2 cells, ascorbic acid induces osteoblastic differentiation and maturation, which are detectable by an increase in ALP activity (18). Thus, medium with or without supplementation of ascorbic acid was used to examine the effects of EMD at various

differentiation stages of ST2 cells. ALP activity was measured using an ALP B-test Wako kit (Wako Chemical Co., Osaka, Japan) based on the method of Lowry-Bessey (24). Fifty microliters of the cell homogenate, part of the sample prepared for DNA measurement, was incubated with the assay buffer at 37°C and the solution was spectrophotometrically measured at 405 nm.

Measurement of mineralized nodule (MN) formation

Twenty-four-well plates were treated with EMD as described above. KUSA/A1 cells were inoculated into 24-well plates at a cell density of 5×10^3 cells/cm^2 and cultured. On d 10, the cultures were fixed with methanol and stained with Alizarin Red S. The stained image was acquired with a densitometor (GS-670, Bio-Rad) and analyzed for MN area by NIH Image 1.61 (National Institutes of Health, Bethesda, MD, USA) on a Macintosh computer.

Gelatin zymography

Substrate gel electrophoresis (zymography) was performed to identify the effect of EMD on the MMP production of KUSA/A1 cells. Culture dishes (35 mm) were treated with EMD as described above. KUSA/A1 cells were inoculated at a cell density of 5×10^3 cells/cm^2, and cultured. On d 4 and 7, KUSA/A1 cells were washed three times with PBS (–), and cultured in serum-free α-MEM for 24 h. The conditioned media was then collected and centrifuged at $1500 \times g$ for 5 min. All supernatants were diluted in a non-reducing sodium dodecyl sulfate-polyacrylamide gel electrophoresis (SDS-PAGE) buffer. The volume of each sample applied to the gel was adjusted depending on the number of cells, which was counted in the corresponding plate after trypsin treatment. The samples were electrophoresed on 15% SDS-polyacrylamide gels containing 2 mg/ml gelatin under non-reducing conditions. After electrophoresis, the gels were washed twice with 2.5% Triton X-100 for 1 h and then incubated in 50 mM Tris-HCl, pH 7.5 containing 5 mM $CaCl_2$, 0.02% NaN_3, 200 nM NaCl and 1 μM $ZnCl_2$ overnight at 37°C. The gels were stained with Coomassie Brilliant Blue R-250. This was followed by destaining.

Northern blot analysis

KUSA/A1 cells were inoculated onto 100-mm dishes treated with EMD, at a cell density of 5×10^3 cells/cm^2 and cultured. On d 4, 7 and 10, the total RNA of the cultures was extracted using an RNA extraction solution (RNAzol B, Biotecx Laboratories, TX, USA), which is based on the guanidine phenol/chloroform method (25). For Northern analysis, 10 μg of each total RNA was electrophoresed on 1.2% agarose gels, stained with ethidium bromide and transferred to nylon membranes (Zeta-Probe, Bio-Rad, CA, USA), using the capillary elution method. After prehybridization, hybridization with [^{32}P]-labeled cDNA was carried out overnight at 42°C. The following cDNA probes were used: a 900-base pair *Pst*I fragment of pα2R2 (α2 chain of rat type I collagen, COL I) (26); a 984-base pair *Hin*dIII fragment of mouse 2ar (osteopontin, OPN) (27); a 912-base pair of rat bone sialoprotein (BSP) (28); a 488-base pair *Eco*RI–*Pst*I fragment of mouse osteocalcin (OC) (29); cDNA of TGF-β1, nucleotide position from 693 to 1217 (30), was prepared by reverse transcription-polymerase chain reaction technique (RT-PCR) from mouse bone mRNA. This DNA fragment was inserted into a pBluescript SK (+) (Strategene Cloning Systems, La Jolla, CA, USA). The hybridized membranes were exposed to Kodak X-OMAT films.

In vivo activity

Twelve-week-old male Wistar rats were anesthetized by intramuscular injection of pentobarbital. An incision was made into the soft tissue, including the periosteum, and the bone surface was exposed. Full-thickness trephine defects (3.8 mm diameter) were created in the bilateral parietal bone. A lyophilized pellet, a 100 μl of 1% bovine atelocollagen (KOKEN Co., Tokyo, Japan) with or without 1 mg EMD, was inserted into the skull defect on the experimental (right-hand) side. The left side skull defect (control) was not filled. Furthermore, to examine the possibility of the involvement of EMD in ectopic bone formation, a pellet of each type was also placed into the hind thigh muscle. Four animals were used for each group described above. Two weeks after the surgical operation, the rats were sacrificed, and the tissues around the operation site were taken and fixed with 10% buffered formalin. To evaluate new bone formation, soft X-ray photographs were taken. Photographic images were acquired with a densitometor (GS-670, Bio-Rad) and analyzed with NIH image 1.61 software on a Macintosh computer. The samples were embedded in methyl methacrylate resin, and ground sections containing the central region of the bone defect were prepared and stained with toluidine blue.

Statistical methods

Numerical data were presented as mean plus one standard deviation. One way analysis of variance (ANOVA) with Fisher's PLSD test was used for multiple comparisons to compare with the control. The probability level of $P < 0.05$ was regarded as statistically significant.

Results

Cell proliferation

In DNA measurements, EMD did not affect ST2 cell growth (data not shown), whereas it stimulated KUSA/A1 cell growth in a concentration-dependent manner (Fig. 1A). When KUSA/A1 cells were inoculated at a cell density of 10^3 cells/cm^2, the cells reached the confluent stage at d 6. The stimulatory effect of EMD on KUSA/A1 cell proliferation was also revealed in the BrdU incorporation assay. These stimulatory effects were observed within 20 days. As shown in Fig. 1(B), EMD stimulated the proliferation of KUSA/A1 cells in a concentration-dependent manner at three different time points: d 4, 8 and 14.

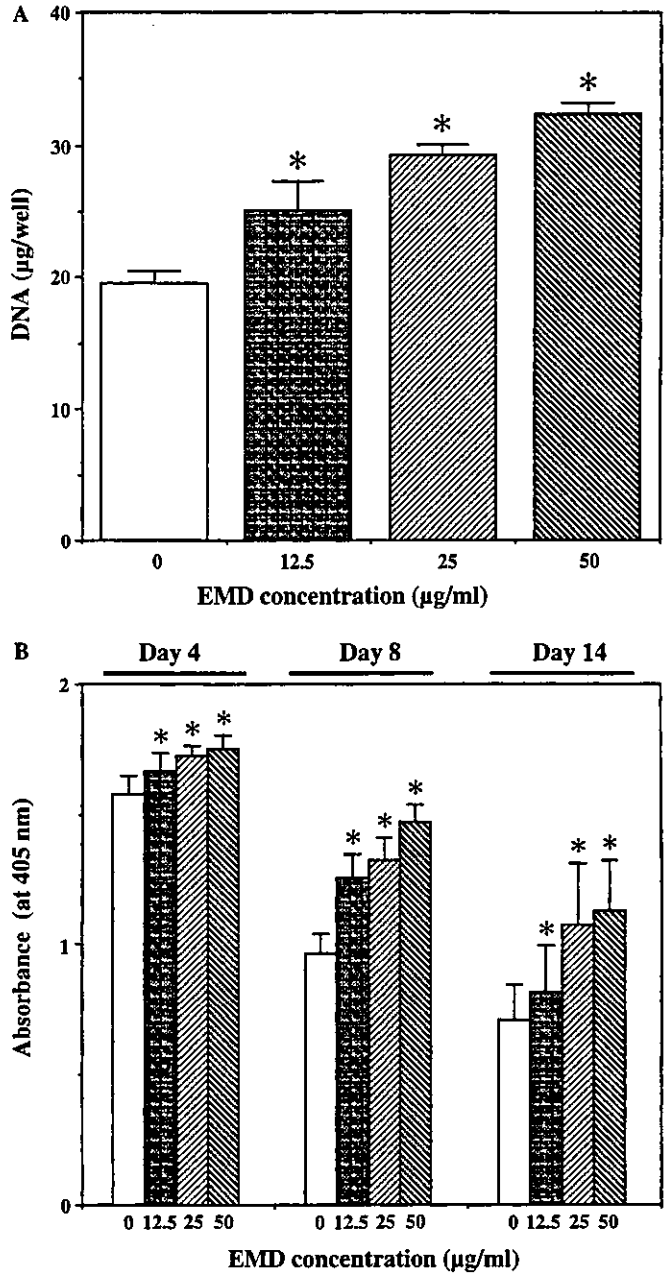

Fig. 1. Effect of EMD on proliferation of KUSA/A1 cells. KUSA/A1 cells were cultured in various concentrations of EMD. Cellular proliferation was analyzed by DNA measurement at d 10 (A) and by BrdU incorporation at d 4, 8 and 14 (B). Data are presented as the mean + SD. $n = 4$ (A) and $n = 6$ (B). *Significantly different from the control at $P < 0.05$.

ALP activity

In ST2 cells, ALP activity was stimulated by EMD in a concentration-dependent manner when culture medium was supplemented with ascorbic acid (Fig. 2A). However, when the culture medium was not supplemented with ascorbic acid, ALP activity of ST2 cells was relatively low, and the EMD stimulatory effect on ALP activity was not observed under this culture condition. In KUSA/A1 cells, EMD stimulated ALP activity in a concentration-dependent manner (Fig. 2B).

MN formation

EMD stimulated MN area of KUSA/A1 cells in a concentration-dependent manner (Fig. 3). Under phase contrast microscopy, the morphology of KUSA/A1 cells was fibroblastic and gradually grew into multiple layers of cells (data not shown). Part of the cell layer became dense and started to mineralize at d 9 or 10. In the EMD-treated culture of KUSA/A1 cells, a thick cell layer with matrix accumulation was evident compared to the control culture.

MMP activity

After the KUSA/A1 cells had been treated with EMD, aliquots of conditioned medium were electrophoresed on SDS-polyacrylamide gels containing gelatin. As shown in Fig. 4, proteolytic degradation of the gelatin appeared as one weak band, and two clear bands (92, 72 and 67 kDa), were detected. EMD stimulatory effect on the expression of these bands was observed on d 4. On d 7, EMD stimulated the expression of 72 and 67 kDa bands, whereas EMD inhibited 92 kDa band expression. To confirm that this MMP activity was derived from the cells rather than from the EMD, the medium from a plate which had not been inoculated with cells was analyzed. Zymography of this sample did not produce any bands (data not shown), indicating that the MMP activity derived from the KUSA/A1 cells, not the EMD.

Northern blotting

In the culture condition for mRNA expression analysis, KUSA/A1 cells reached a confluence on d 4 and MN appeared on d 8 or 9. RNA was extracted from the culture on d 4, 7 and 10, and hybridized with various osteoblastic cDNA probes. The mRNA expression of COL I, OPN, BSP, TGF-β1 and OC is shown in Fig. 5. EMD enhanced mRNA expression of both COL I and OPN on d 4 and 7. However, the level of the enhancement was different at each time point. EMD did not affect BSP mRNA expression. The expression of TGF-β1 was not detected until d 7,

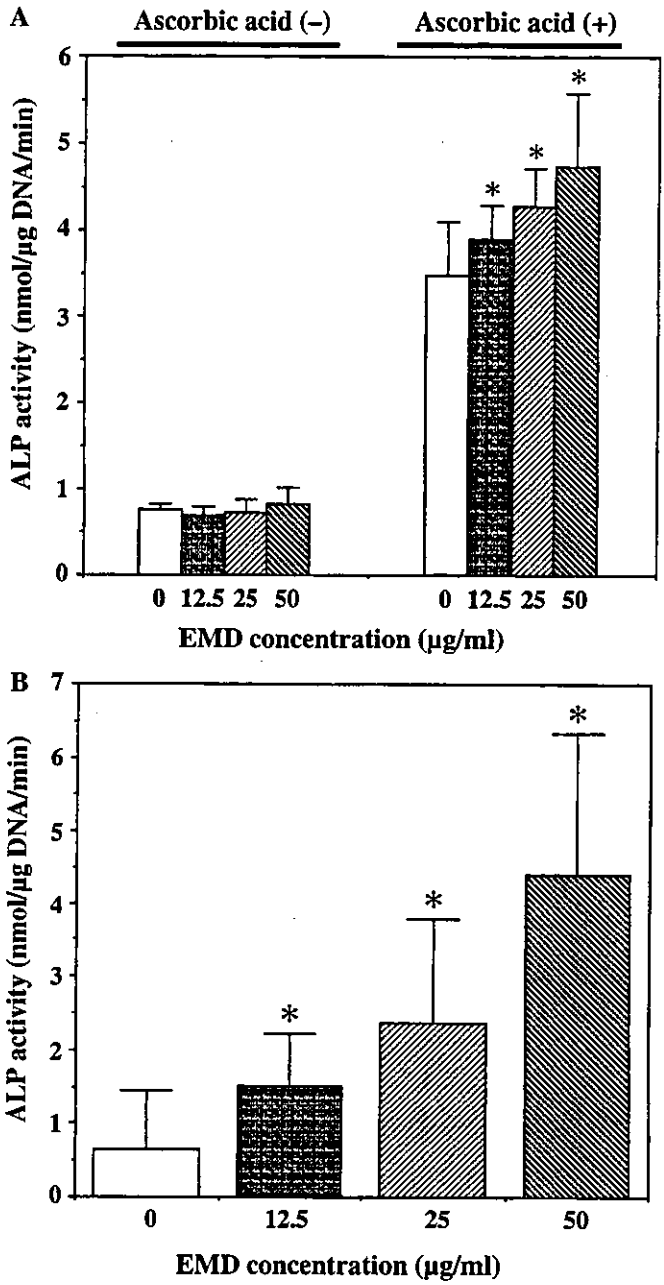

Fig. 2. Effect of EMD on ALP activity of ST2 cells (A) and KUSA/A1 cells (B). The cells were cultured in various concentrations of EMD; ALP activity of ST2 cells and KUSA/A1 cells was measured at d 16 and d 10, respectively. In ST2 cell culture, the medium with or without ascorbic acid was used. Data are presented as the mean + SD ($n = 4$). *Significantly different from the controls at $P < 0.05$.

and EMD enhanced TGF-β1 expression on d 7 and 10. The expression of OC was not detectable on d 4 or 7, and low expression of OC was observed on d 10. Extensive stimulation of OC expression by EMD treatment was observed on d 10.

EMD implantation

As shown in Fig. 6(A), the new bone formation in the bone defect appeared as radio-opaque areas in a soft X-ray photograph, and EMD stimulated new bone formation. The radio-opaque area of untreated-defect and defect treated with atelocollagen was approximately 10% and 35% of the original defect, respectively (Fig. 6B). In the group treated with atelocollagen and EMD, the radio-opaque area occupied 70% of the original bone defect (Fig. 6B). Histologically, newly formed mineralized bone and numerous migratory cells were evident in the pellets containing EMD (Fig. 6C). Two weeks after their implantation into the muscle, the pellets containing EMD had not induced mineralized tissue (data not shown).

Discussion

Commercially available EMD is a material extracted by acetic acid from porcine enamel matrix. The main component of EMD is amelogenin (3), although enamel matrix also contains other enamel proteins such as ameloblastin (known as amelin and sheathlin), and enamelin; it also contains several proteinases (31, 32). Since amelogenin is very hydrophobic and insoluble in water at neutral pH, EMD has similar solubility characteristics. In a clinical situation, immediately after EMD application, EMD probably forms aggregates on the denuded dentin surface. In the present study, EMD was precipitated after addition to the culture medium, after which the cells were inoculated. This method mimics the clinical situation and the same method has already been applied in other cell culture studies (13, 15).

PDL is a thin connective tissue between alveolar bone and cementum. Previous histological studies (33, 34) strongly suggest that PDL contains progenitor cells, specifically cementoblasts and osteoblasts. This concept is also supported by *in vitro* studies. In cell culture, PDL cells demonstrate osteoblastic characteristics such as high ALP activity (35, 36), cAMP production in response to parathyroid hormone and prostaglandin E_2 (36–38), and an ability to form MN (39, 40). A previous study has shown that EMD stimulates the proliferation, ALP activity, matrix production and MN formation of PDL cells (13), which correspond closely with the

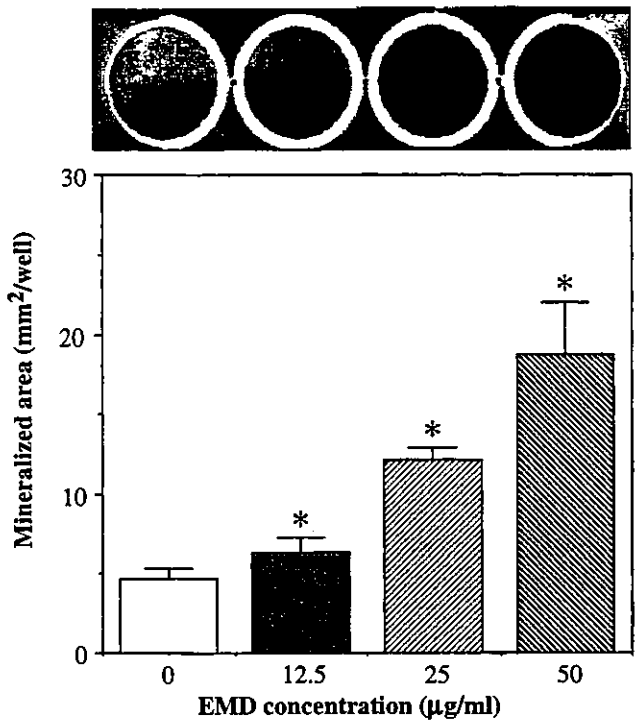

Fig. 3. Effect of EMD on MN formation of KUSA/A1 cells. KUSA/A1 cells were cultured in various concentrations of EMD. At d 10, the culture was fixed, stained with Alizarin Red S, and then mineralized area was measured. Stained image was presented in the upper panel. Data are presented as the mean + SD ($n = 6$). *Significantly different from the control at $P < 0.05$.

EMD stimulatory effect in periodontal tissue regeneration. Thus, EMD probably acts on cells of cementoblast or osteoblast lineage in PDL.

In the present study, we examined the effects of EMD on two different osteoblastic cells: ST2 cells and KUSA/A1 cells. ST2 cells are derived from mouse bone marrow and they differentiate to adipocytes or osteoblasts depending on culture conditions (18, 41). ST2 cells respond well to BMP-2, which subsequently induces high ALP activity (18). Supplementation with ascorbic acid leads ST2 cells to demonstrate high ALP activity (18). KUSA/A1 cells also originate from mouse bone marrow. They have the ability to form bone-like tissue when transplanted into mice, and also an ability to form MN in culture (19) and in the present study, KUSA/A1 cells could form MN very quickly and had high ALP activity immediately after the confluence. Therefore, compared to ST2 cells, KUSA/A1 cells are highly committed to osteoblastic linage and high osteoblastic activity.

In previous studies, the EMD effect on cellular proliferation has been shown to vary according to cell type. For example, EMD stimulates the proliferation of PDL cells and gingival fibroblasts (13, 15). However, EMD inhibits the proliferation of SCC25 cells (cells from human squamous cell carcinoma of the tongue) (17), whereas EMD does not affect the proliferation of other epithelial cells or HT1028 cells (13). The effect of EMD on cellular proliferation of several osteoblastic cells has been reported; this also suggests a diversity of cell responses to EMD (16, 42). In the present study, EMD stimulated KUSA/A1 cell proliferation although it did not affect ST2 cell proliferation which would confirm this. Thus, the effect of EMD on cellular proliferation depends on cell type.

Previous studies have shown that EMD effects on cellular ALP activity also depend on cell type. EMD stimulates the ALP activity of PDL cells, gingival fibroblasts (15), and some osteoblastic cells (normal human osteoblast-like cells and MG63 cells), whereas it does not stimulate ALP activity in 2T9 cells (16), an immature osteoprogenitor cell line. In the present study, when ST2 cells were induced by ascorbic acid to demonstrate osteoblastic differentiation and maturation, EMD stimulated the ALP activity of these ST2 cells. However, EMD did not affect the ALP activity of ST2 cells cultured without ascorbic acid supplementation. Furthermore, EMD stimulated the ALP activity of KUSA/A1 cells, which induced by supplementation of β-glycerophoshate. Thus, EMD could act on osteoblastic cells by increasing their ALP activity, but EMD could not induce initial production of ALP.

BMP-2 induces ALP activity in ST2 cells without ascorbic acid supplementation (18), whereas EMD did not induce ALP activity in ST2 cells without ascorbic acid supplementation. Intramuscular implantation of BMP-2 induces ectopic bone, whereas the pellets containing EMD did not induce ectopic bone formation in the present study. Boyan and her collaborators (20) have also reported that implantation of demineralized freeze-dried bone containing EMD in mouse muscle did not induce ectopic bone formation. Thus, the EMD does not have BMP-like osteoinductive activity.

EMD stimulated MN formation in KUSA/A1 cells. Although the mechanism and process of bone mineralization are not fully understood, it is thought that MN formation is the accumulated result of osteoblastic phenotype expression. In the present study, an increase in cell number was evident in the EMD-treated culture, which might partly contribute to the increase in MN. EMD stimulated the expression of osteoblastic phenotypes, including ALP activity and the production of some matrices. The stimulation of these phenotype expressions could significantly contribute to the increase in MN.

Matrix metalloproteinases (MMPs) are a family of related proteolytic enzymes that contain collagenases,

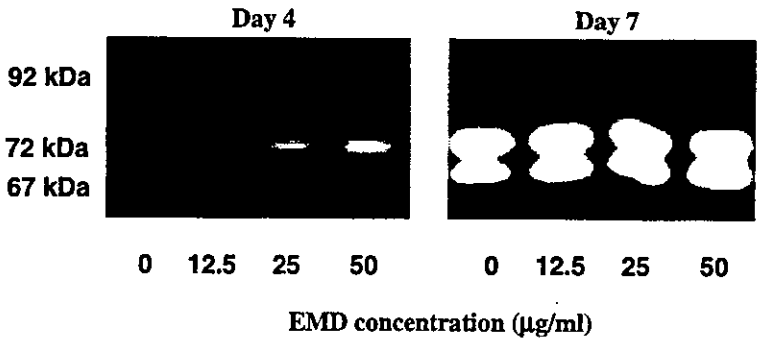

Fig. 4. Effect of EMD on MMP production in KUSA/A1 cells. KUSA/A1 cells were cultured in various concentrations of EMD. At d 4 and 7, medium was changed, conditioned medium was collected after 24 h, and then analyzed in gelatin zymography. The sample amount applied to the gels was corrected with the cell number of each sample. Thus, the intensity of the band means the relative MMP production of approximately same number of cells.

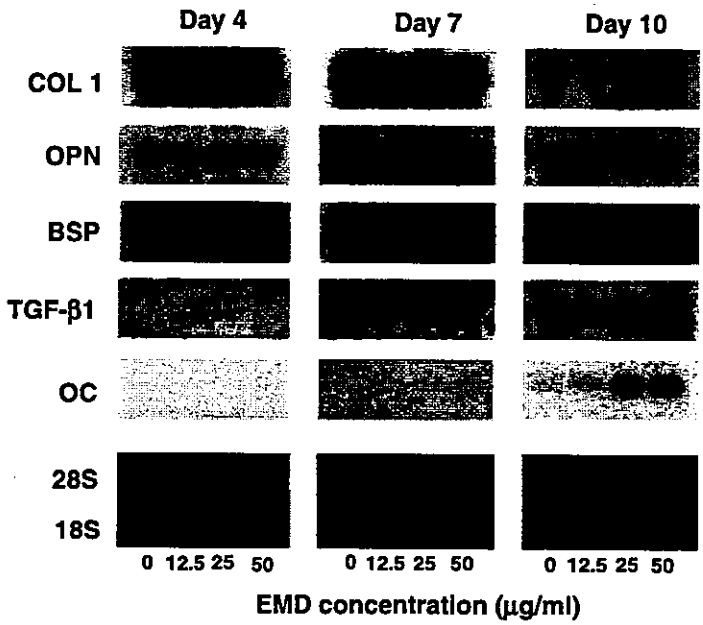

Fig. 5. Effect of EMD on mRNA expression of osteoblastic phenotypes in KUSA/A1 cells. mRNA expression of type I collagen (COL I), osteopontin (OPN), bone sialoprotein (BSP), transforming growth factor beta 1 (TGF-β1) and osteocalcin (OC) was analyzed in Northern blotting. The lowest panel represents the relative amount of the total RNA loaded in each lane.

gelatinases and stromelysins. The expression of MMPs as mediators of extracellular matrix remodeling appears critical to many growing or regenerating tissues (43–46). It is known that osteoblasts secrete MMP-1, 2, 3, 9, 10 and 13 (47–49), and these MMPs all have gelatinolytic activity with the exception of MMP-13. The present zymographic results showed three bands at 92, 72 and 67 kDa. Based on their molecular weight, they are probably attributable to a proenzyme form of MMP-9 and MMP-2, and an active form of MMP-2, respectively. MMP-2 and -9 are able to degrade native and denatured interstitial collagens as well as the basement membrane collagen (50). EMD stimulated MMP-2 production on d 4 and 7. In the EMD-treated culture of KUSA/A1 cells, a thick cell layer with matrix accumulation was evident. Thus, it is likely that EMD compensatively stimulates matrix production, although EMD also stimulates MMP production and matrix degradation. On d 7, the production of MMP-9 was inhibited by EMD. It has been reported that ALP-transfected osteosarcoma cells with high ALP activity inhibit the secretion of MMP-9 (51). The decrease in MMP-9 might correspond to the elevation of ALP in KUSA/A1 cells on d 7, although the physiological significance of this phenomenon is not clear.

It has been reported that EMD enhances extracellular matrix production, such as collagen and fibronectin, and TGF-β1 secretion in PDL cells (13–15). EMD also increases the level of TGF-β1 but has no effect on the production of collagen in the culture of osteoblastic MG63 cells (16). In KUSA/A1 cells, EMD strongly enhanced mRNA expression of COL I on d 4, TGF-β1 and OC on d 10. Although enhancement of MMP by EMD was detected by zymography, we speculate that the enhancement of the matrix proteins and TGF-β1 probably overcame the matrix degradation, resulting in matrix accumulation and the increase in MN formation.

Several *in vivo* experiments have demonstrated that EMD stimulates regeneration of the periodontal tissue including alveolar bone (5–7) and regeneration of bone defect in the femur (21). In these *in vivo* experiments, a variety of cells participate in bone regeneration. Thus, in the present study, we used calvarial bone defect model to clarify the direct effect of EMD on bone regeneration because the regeneration process of this bone defect model is probably simple. EMD stimulated new bone formation in a rat skull bone defect; however, EMD did not induce ectopic bone formation when it was intramuscularly implanted. Histologically, an increase in number of cells in the EMD pellets was evident. These cells in the pellets might have originated from the periosteum and endosteum of the bony rim of the defect. Since EMD enhances the

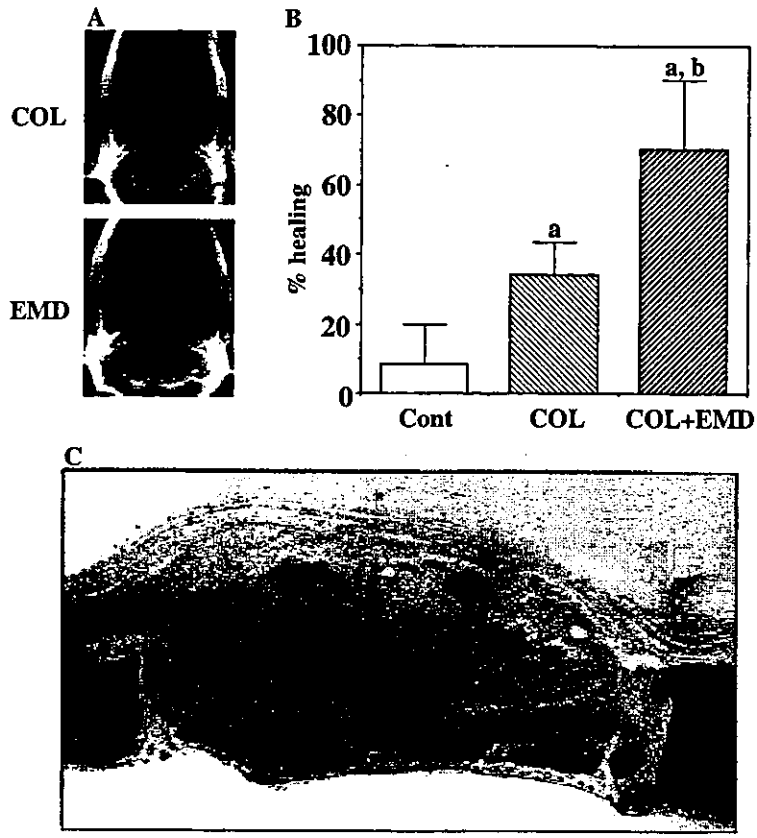

Fig. 6. Effect of EMD on healing of rat skull defect. (A) Soft X-ray photographs were taken at 2 weeks after the operation. Right defects were filled with atelocollagen (upper; COL) or with atelocollagen containing EMD (lower; COL + EMD). Left side (upper and lower) was control (filled with nothing). (B) Healing of the skull defects after various treatments. Radiopacity area of defects was measured and calculated the percentage of their occupied area of the defect. Data are presented as the mean + SD ($n = 4$: each experimental groups. $n = 8$: control group). Significantly different from the control or COL group at $^{a}P < 0.05$, $^{b}P < 0.05$, respectively. (C) Histological section of EMD treated group. At 2 weeks after the operation, new formed bone and mineralized deposit were observed in implantation of EMD (toluidine blue staining).

migration of PDL cells in the *in vitro* wound healing model (14), a similar phenomenon could have occurred at the healing site of the skull bone defect treated with EMD.

Veis *et al.* (52) have reported that short forms of the spliced products of rat amelogenin induce chondrogenic phenotypes in cultures of embryonic rat muscle cells, and that implantation of these recombinant amelogenins in muscle induces the formation of ectopic mineralized tissue. However, in the present study, EMD pellets did not induce such ectopic mineralization. It is certain that EMD contains various types of amelogenins; however, it is unlikely that EMD contains similar molecules of inducing ectopic mineralization. Boyan and her collaborators (20) have reported that EMD stimulates the bone formation ectopically induced by BMP although EMD does not have BMP-like osteoinductive activity. Their findings and our *in vivo* results indicate that EMD has an ability to stimulate the bone formation that is induced by BMP or during the bone regeneration process.

In conclusion, although the effects of EMD on osteoblastic cells are complex, the overall effect of EMD on osteoblastic cells is stimulatory rather than inhibitory, which could contribute favorably to bone regeneration. EMD itself is not an osteoinductive material like BMPs; however, it may have potential therapeutic as a material for bone regeneration.

Acknowledgements

This study was supported by a Grant-in Aid from the Japanese Ministry of Education, Culture, Sports, Science and Technology (11470460) and the Japan Society for the Promotion of Science (96I00205).

References

1. Slavkin HC. Towards a cellular and molecular understanding of periodontics: Cementogenesis revisited. *J Periodontol* 1976;47:249–255.
2. Hammarström L. Enamel matrix, cementum development and regeneration. *J Clin Periodontol* 1997;24:658–668.
3. Hammarström L, Heijl L, Gestrelius S. Periodontal regeneration in a buccal dehiscence model in monkeys after application of enamel matrix proteins. *J Clin Periodontol* 1997;24:669–677.
4. Heijl L. Periodontal regeneration with enamel matrix derivative in one human experimental defect. A case report. *J Clin Periodontol* 1997;24:693–696.
5. Araujo MG, Lindhe J. GTR treatment of degree III furcation defects following application of enamel matrix proteins. An experimental study in dogs. *J Clin Periodontol* 1998;25:524–530.
6. Sculean A, Donos N, Brecx M, Reich E, Karring T. Treatment of intrabony defects with guided tissue regeneration and enamel-matrix-proteins – An experimental study in monkeys. *J Clin Periodontol* 2000;27:466–472.
7. Sculean A, Donos N, Reich E, Karring T, Brecx M. Regeneration of oxytalan fibres in different types of periodontal defects: a histological study in monkeys. *J Periodont Res* 1998;33:453–459.
8. Heden G, Wennstrom J, Lindhe J. Periodontal tissue alterations following Emdogain treatment of periodontal sites with angular bone defects. A series of case reports. *J Clin Periodontol* 1999;26:855–860.
9. Heijl L, Heden G, Svardstrom G, Ostgren A. Enamel matrix derivative (EMDOGAIN) in the treatment of intrabony periodontal defects. *J Clin Periodontol* 1997;24:705–714.
10. Rasperini G, Ricci G. Surgical technique for treatment of infrabony defects with enamel matrix derivative (Emdogain): 3 case reports. *Int J Periodontics Restorative Dent* 1999;19:578–587.

11. Sculean A, Reich E, Chiantella GC, Brecx M. Treatment of intrabony periodontal defects with an enamel matrix protein derivative (Emdogain). a report of 32 cases. *Int J Periodontics Restorative Dent* 1999;**19**:157–163.
12. Sculean A, Donos N, Karring T *et al.* Healing of human intrabony defects following treatment with enamel matrix proteins or guided tissue regeneration. *J Periodont Res* 1999;**34**:310–322.
13. Gestrelius S, Andersson C, Lidstrom D, Hammarström L, Somerman M. *In vitro* studies on periodontal ligament cells and enamel matrix derivative. *J Clin Periodontol* 1997;**24**:685–692.
14. Hoang AM, Oates TW, Cochran DL. *In vitro* wound healing responses to enamel matrix derivative. *J Periodontol* 2000;**71**:1270–1277.
15. Van der Pauw MT, Van den Bos T, Everts V, Beertsen W. Enamel matrix-derived protein stimulates attachment of periodontal ligament fibroblasts and enhances alkaline phosphatase activity and transforming growth factor beta 1 release of periodontal ligament and gingival fibroblasts. *J Periodontol* 2000;**71**:31–43.
16. Schwartz Z, Carnes DL Jr, Boyan BD *et al.* Porcine fetal enamel matrix derivative stimulates proliferation but not differentiation of pre-osteoblastic 2T9 cells, inhibits proliferation and stimulates differentiation of osteoblast-like MG63 cells, and increases proliferation and differentiation of normal human osteoblast NHOst cells. *J Periodontol* 2000;**71**:1287–1296.
17. Kawase T, Okuda K, Yoshie H, Burns DM. Cytostatic action of enamel matrix derivative (EMDOGAIN®) on human oral squamous cell carcinoma-derived SCC25 epithelial cells. *J Periodont Res* 2000;**35**:291–300.
18. Otsuka E, Yamaguchi A, Hirose S, Hagiwara H. Characterization of osteoblastic differentiation of stromal cell line ST2 that is induced by ascorbic acid. *Am J Physiol* 1999;**277**:C132–C138.
19. Umezawa A, Maruyama T, Segawa K, Shadduck RK, Waheed A, Hata J. Multipotent marrow stromal cell line is able to induce hematopoiesis *in vivo*. *J Cell Physiol* 1992;**151**:197–205.
20. Boyan BD, Weesner TC, Schwartz Z *et al.* Porcine fetal enamel matrix derivative enhances bone formation induced by demineralized freeze dried bone allograft *in vivo*. *J Periodontol* 2000;**71**:1278–1286;.
21. Kawana F, Sawae Y, Sasaki T *et al.* Porcine enamel matrix derivative enhances trabecular bone regeneration during wound healing of injured rat femur. *Anat Rec* 2001;**264**:438–446.
22. Labarca C, Paigen K. A simple, rapid, and sensitive DNA assay procedure. *Anal Biochem* 1980;**102**:344–352.
23. Porstmann T, Ternynck T, Avrameas S. Quantitation of 5-bromo-2-deoxyuridine incorporation into DNA: an enzyme immunoassay for the assessment of the lymphoid cell proliferative response. *J Immunol Meth* 1985;**82**:169–179.
24. Bessey OA, Lowry OH, Breck MJ. A method for the rapid determination of alkaline phosphatase with five cubic millimeters of serum. *J Biol Chem* 1946;**164**:312–326.
25. Chomczynski P, Sacchi N. Single-step method of RNA isolation by acid guanidinium thiocyanate-phenol-chloroform extraction. *Anal Biochem* 1987;**162**:156–159.
26. Genovese C, Rowe D, Kream B. Construction of DNA sequences complementary to rat alpha 1 and alpha collagen mRNA and their use in studying the regulation of type I collagen synthesis by 1,25-dihydroxyvitamin D. *Biochemistry* 1984;**23**:6210–6216.
27. Nomura S, Wills AJ, Edwards DR, Heath JK, Hogan BL. Developmental expression of 2ar (osteopontin) and SPARC (osteonectin) as revealed by in situ hybridization. *J Cell Biol* 1988;**106**:441–450.
28. Chen JK, Shapiro HS, Wrana JL, Reimers S, Heersche JN, Sodek J. Localization of bone sialoprotein (BSP) expression to sites of mineralized tissue formation in fetal rat tissues by in situ hybridization. *Matrix* 1991;**11**:133–143.
29. Celeste AJ, Rosen V, Buecker JL, Kriz R, Wang EA, Wozney JM. Isolation of the human gene for bone gla protein utilizing mouse and rat cDNA clones. *EMBO J* 1986;**5**:1885–1890.
30. Derynck R, Jarrett JA, Chen EY, Goeddel DV. The murine transforming growth factor-beta precursor. *J Biol Chem* 1986;**261**:4377–4379.
31. Fincham AG, Hu Y, Lau EC, Slavkin HC, Snead ML. Amelogenin post-secretory processing during biomineralization in the postnatal mouse molar tooth. *Arch Oral Biol* 1991;**36**:305–317.
32. Termine JD, Belcourt AB, Christner PJ, Conn KM, Nylen MU. Properties of dissociatively extracted fetal tooth matrix proteins. I. Principal molecular species in developing bovine enamel. *J Biol Chem* 1980;**255**:9760–9768.
33. Buser D, Warrer K, Karring T. Formation of a periodontal ligament around titanium implants. *J Periodontol* 1990;**61**:597–601.
34. Herr Y, Matsuura M, Lin WL, Genco RJ, Cho MI. The origin of fibroblasts and their role in the early stages of horizontal furcation defect healing in the beagle dog. [published erratum appears in *J Periodontol* 66: 915–923; 1995.] *J Periodontol* 1995;**66**:716–730.
35. Nojima N, Kobayashi M, Shionome M, Takahashi N, Suda T, Hasegawa K. Fibroblastic cells derived from bovine periodontal ligaments have the phenotypes of osteoblasts. *J Periodont Res* 1990;**25**:179–185.
36. Piche JE, Carnes DL Jr, Graves DT. Initial characterization of cells derived from human periodontia. *J Dent Res* 1989;**68**:761–767.
37. Nohutcu RM, McCauley LK, Horton JE, Capen CC, Rosol TJ. Effects of hormones and cytokines on stimulation of adenylate cyclase intracellular calcium concentration in human and canine periodontal-ligament fibroblasts. *Arch Oral Biol* 1993;**38**:871–879.
38. Rao LG, Moe HK, Heersche JN. *In-vitro* culture of porcine periodontal ligament cells: response of fibroblast-like and epithelial-like cells to prostaglandin E1, parathyroid hormone and calcitonin and separation of a pure population fibroblast-like cells. *Arch Oral Biol* 1978;**23**:957–964.
39. Groeneveld MC, Everts V, Beertsen W. Formation of afibrillar acellular cementum-like layers induced by alkaline phosphatase activity from periodontal ligament explants maintained *in vitro*. *J Dent Res* 1994;**73**:1588–1592.
40. Ramakrishnan PR, Lin WL, Sodek J, Cho MI. Synthesis of noncollagenous extracellular matrix proteins during development of mineralized nodules by rat periodontal ligament cells *in vitro*. *Calcif Tissue Int* 1995;**57**:52–59.
41. Yamaguchi A, Ishizuya T, Yoshiki S *et al.* Effects of BMP-2, BMP-4, and BMP-6 on osteoblastic differentiation of bone marrow-derived stromal cell lines, ST2 and MC3T3–G2/PA6. *Biochem Biophys Res Commun* 1996;**220**:366–371.
42. Tokiyasu Y, Takata T, Saygin E, Somerman M. Enamel factors regulate expression of genes associated with cementoblasts. *J eriodontol* 2000;**71**:1829–1839.
43. Chin JR, Werb Z. Matrix metalloproteinases regulate morphogenesis, migration and remodeling of epithelium, tongue skeletal muscle and cartilage in the mandibular arch. *Development* 1997;**124**:1519–1530.
44. Johansson N, Saarialho-Kere U, Kahari VM *et al.* Collagenase-3 (MMP-13) is expressed by hypertrophic chondrocytes, periosteal cells, and osteoblasts during human fetal bone development. *Dev Dyn* 1997;**208**:387–397.
45. La Fleur M, Underwood JL, Rappolee DA, Werb Z. Basement membrane and repair of injury to peripheral nerve: defining a potential role for macrophages, matrix metalloproteinases, and tissue inhibitor of metalloproteinases-1. *J Exp Med* 1996;**184**:2311–2326.
46. Yang EV, Bryant SV. Developmental regulation of a matrix metalloproteinase during regeneration of axolotl appendages. *Dev Biol* 1994;**166**:696–703.